catalysts

MDPI

Supporting Information

Replacing Pyridine with Pyrazine in Molecular Cobalt Catalysts: Effects on Electrochemical Properties and Aqueous H_2 Generation

Lars Kohler [1], Andrea M. Potocny [1], Jens Niklas [1], Matthias Zeller [2], Oleg G. Poluektov [1] and Karen L. Mulfort [1,*]

[1] Division of Chemical Sciences and Engineering, Argonne National Laboratory, Lemont IL 60439, USA; larskohler227@gmail.com (L.K.); ampotocny@anl.gov (A.M.P.); jniklas@anl.gov (J.N.); oleg@anl.gov (O.G.P.)
[2] Department of Chemistry, Purdue University, West Lafayette, IN 47907, USA; zeller4@purdue.edu
* Correspondence: mulfort@anl.gov

Contents

Description of synthesis

Unless described below, all reagents and solvents were obtained from commercial sources and used as received.

6-(Pyridin-2-yl)pyrazin-2-amine (1): 6-Chloropyrazin-2-amine (2.00 g, 23.16 mmol), $Pd(PPh_3)_4$ (1.34 g, 1.16 mmol) and 2-(tributylstannyl)pyridine (9.38 g, 25.47 mmol) were dissolved in toluene (120 mL) under nitrogen. The reaction was refluxed for 16 hours. After cooling to 4°C the product was filtered and washed with toluene. The product was isolated in 53 % yield (2.13 g, 12.37 mmol) and used without any further purification. ^{1}H NMR ($CDCl_3$): δ 8.92 (s, 1H); 8.70 (dd, J = 5.0 Hz, J = 1.0 Hz, 1H); 8.21 (dt, J = 8.0 Hz, J = 2.0 Hz, 1H); 8.03 (s, 1H); 7.81 (dt, J = 8.0 Hz, J = 1.5 Hz, 1H); 7.32 (dd, J = 7.5 Hz, J = 1.0 Hz, 1H); 4.63 (s, 2H). ESI-MS (CH_3OH): calcd $[M+H]^+$ 173.08; obsd 173.08.

***N*-(6-(Pyridin-2-yl)pyrazin-2-yl)-[2,2'-bipyridin]-6-amine (2):** 1,1'-Bis(diphenylphosphino)ferrocene (80.5 mg, 0.15 mmol) and bis(dibenzylideneacetone)palladium(0) (66.5 mg, 0.07 mmol) were placed in a Schlenk flask under nitrogen. Dry toluene (10 mL) was added and the solution was stirred for 20 min. 6-(pyridin-2-yl)pyrazin-2-amine (**1**) (500 mg, 2.90 mmol) dissolved in toluene (5 mL) was added followed by a lithium bis(trimethylsilyl)amide in toluene solution (1 M, 3.78 mL, 3.78 mmol) and the resulting orange solution was stirred at room temperature for 30 minutes. 6-Bromo-2,2′-bipyridine (682.6 mg, 2.90 mmol) dissolved in toluene (10 mL) was added and the reaction was stirred for 16 hours at 50°C. Chromatography on silica, eluting with dichloromethane/acetone (5:3 ratio) afforded the product in 57% yield (540 mg, 1.65 mmol). The product was used without any further purification. ^{1}H NMR ($CDCl_3$): δ 9.30 (s, 1H); 9.19 (s, 1H); 8.75 (dt, J = 4.5 Hz, J = 1.0 Hz, 1H); 8.71 (td, J = 3.0 Hz, J = 1.0 Hz, 1H); 8.40 (dd, J = 7.5 Hz, J = 1.0 Hz, 1H); 8.30 (dd, J = 9.0 Hz, J = 1.0 Hz, 1H); 8.07 (dd, J = 7.5 Hz, J = 1.0 Hz, 1H); 7.82-7.88 (m, 3H); 7.52 (d, J = 8.0 Hz, 1H); 7.47 (s, 1H); 7.38 (dt, J = 5.0 Hz, J = 1.0 Hz, 1H); 7.34 (td, J = 7.0 Hz, J = 1.0 Hz, 1H). ESI-MS (CH_3OH): calcd $[M+H]^+$ 327.14; obsd 327.17; calcd $[M+Na]^+$ 349.12; obsd 349.17.

***N*-Butyl-*N*-(6-(pyridin-2-yl)pyrazin-2-yl)-[2,2'-bipyridin]-6-amine (L1):** *N*-(6-(Pyridin-2-yl)pyrazin-2-yl)-[2,2'-bipyridin]-6-amine (**2**) (291.8 mg, 0.90 mmol) and potassium hydroxide (251.1 mg, 4.48 mmol) were placed in a dry Schlenk flask. Dry dimethylsulfoxide (10 mL) was added and the mixture stirred at room temperature for 30 minutes. 1-Bromobutane (193 μL, 1.79 mmol) was added and the reaction was stirred at room temperature for 16 hours. Water (50mL) was added to obtain the product as a very fine precipitate. The precipitate was collected by centrifugation at 16000 rpm for 20 minutes at 4°C. After washing the precipitate with water (2 times) the precipitate was dissolved in dichloromethane. The organic fraction was washed with water and brine, dried over $MgSO_4$, filtered and concentrated. Chromatography on silica, eluting with dichloromethane/20% acetone afforded the product in 85% yield (290 mg, 0.76 mmol). The product was used without any further purification. ^{1}H NMR ($CDCl_3$): δ 9.12 (s, 1H); 8.72 (dt, J = 5.0 Hz, J = 1.0 Hz, 1H); 8.71 (s, 1H); 8.67 (dt, J = 5.0 Hz, J= 1.0 Hz, 1H); 8.31 (tt, J = 7.5 Hz, J = 1.0 Hz, 2H); 8.13 (d, J = 7.0 Hz, 1H); 7.79-7.84 (m, 3H); 7.34 (dd, J = 7.5 Hz, J = 5.0 Hz, 1H); 7.31 (dd, J =7.5 Hz, J = 5.0 Hz, 1H); 7.24 (d, J = 8.0 Hz, 1H); 4.36 (t, J = 7.5 Hz, 2H); 1.86 (pentet, J =7.0 Hz, 2H); 1.49 (sextet, J = 7.5 Hz, 2H); 0.99 (t, J = 7.5 Hz, 3H). ESI-MS (CH_3OH): calcd $[M+H]^+$ 383.20; obsd 383.25; calcd $[M+Na]^+$ 405.18; obsd 405.25.

***N*-Butyl-[2,2'-bipyridin]-6-amine (3):** 6-Bromo-2,2'-bipyridine (2.00 g, 8.51 mmol) and *n*-butylamine (10 mL) were placed in a pressure tube and the reaction was deaerated for 15 minutes. The pressure tube was sealed and the reaction was stirred at 200°C for 24 hours. The reaction mixture was allowed to cool to room temperature and concentrated. Chromatography on silica and eluting with dichloromethane afforded the product as an off-white oil in 99% yield (1.90 g). The product was used without any further purification. ^{1}H NMR ($CDCl_3$): δ 8.65 (dq, J = 5.0 Hz, J = 1.0 Hz, 1H); 8.30 (d, J = 8.0 Hz, 1H); 7.77 (td, J = 7.5 Hz, J = 2.0 Hz, 1H); 7.64 (dd, J = 7.5 Hz, J = 0.5 Hz, 1H); 7.56 (t, J = 8.0 Hz, 1H); 7.24-7.27 (m, 1H); 6.42 (d, J = 8.5 Hz, 1H); 4.58 (s, 1H); 3.35 (q, J = 7.0 Hz, 2H); 1.66 (pentet, J = 7.5 Hz,

2H); 1.47 (sextet, J = 7.5 Hz, 2H); 0.98 (t, J = 7.5 Hz, 3H). ESI-MS (CH_3OH): calcd $[M+H]^+$ 228.15; obsd 228.25.

***N*-(6-Bromopyridin-2-yl)-*N*-butyl-[2,2′-bipyridin]-6-amine (4):** 1,1'-Bis(diphenylphosphino)ferrocene (65.9 mg, 0.12 mmol) and bis(dibenzylideneacetone)palladium(0) (45.5 mg, 0.08 mmol) were placed in a Schlenk flask under nitrogen. Dry toluene (10 mL) was added and the solution was stirred for 20 min. *N*-butyl-[2,2'-bipyridin]-6-amine (**3**) (600 mg, 2.64 mmol) dissolved in toluene (5 mL) was added followed by a lithium bis(trimethylsilyl)amide in toluene solution (1 M, 3.70 mL, 3.70 mmol) and the resulting orange solution was stirred at room temperature for 30 minutes. 2,6-Dibromopyridine (1.25 g, 5.28 mmol) dissolved in toluene (10 mL) was added and the reaction stirred for 16 hours at 50°C. The solvent was evaporated and chromatography on silica, eluting with dichloromethane afforded the product as a solid in 79% yield (800 mg, 2.09 mmol). The product was used without any further purification. ^{1}H NMR ($CDCl_3$): δ 8.67 (dd, J = 5.0 Hz, J = 1.0 Hz, 1H); 8.32 (d, J = 8.0 Hz, 1H); 8.07 (d, J = 7.5 Hz, 1H); 7.79 (td, J = 7.5 Hz, J = 2.0 Hz, 1H); 7.71 (t, J = 8.0 Hz, 1H); 7.31 (t, J = 7.5 Hz, 1H); 7.29 (dt, J = 4.5 Hz, J = 1.5 Hz, 1H); 7.20 (d, J = 8.5 Hz, 1H); 7.06 (d, J = 8.5 Hz, 1H); 6.97 (d, J = 7.5 Hz, 1H); 4.27 (t, J = 7.5 Hz, 2H); 1.75 (pentet, J = 6.0 Hz, 2H); 1.42 (sextet, J = 7.5 Hz, 2H); 0.96 (t, J = 7.5 Hz, 3H). ESI-MS (CH_3OH): calcd $[M+H]^+$ 383.09; obsd 383.17; calcd $[M+Na]^+$ 405.07; obsd 405.17.

***N*-butyl-*N*-(6-(pyrazin-2-yl)pyridin-2-yl)-[2,2'-bipyridin]-6-amine (L2):** *N*-(6-Bromopyridin-2-yl)-*N*-butyl-[2,2'-bipyridin]-6-amine (**4**) (800 mg, 2.09 mmol), $Pd(PPh_3)_4$ (120.6 mg, 0.10 mmol) and 2-(tributylstannyl)pyrazine (924.6 mg, 2.51 mmol) were dissolved in toluene (30 mL) under nitrogen. The reaction was refluxed for 16 hours. After cooling to room temperature the reaction was quenched with water and the product was extracted with dichloromethane. After extraction with hydrochloric acid (4M), the aqueous layer was neutralized with aqueous ammonia and then again extracted with dichloromethane. The organic fraction was dried with $MgSO_4$, filtered and concentrated. The product was isolated in 95% yield (760 mg, 1.99 mmol) and used without any further purification. ^{1}H NMR ($CDCl_3$): δ 9.60 (d, J = 1.5 Hz, 1H); 8.68 (ddd, J = 5.0 Hz, J = 1.5 Hz, J = 1.0 Hz, 1H); 8.61 (dd, J = 2.5 Hz, J = 1.5 Hz, 1H); 8.57 (d, J = 2.5 Hz, 1H); 8.36 (d, J = 8.0 Hz, 1H); 8.06 (d, J = 7.0 Hz, 1H); 7.94 (d, J = 7.0 Hz, 1H); 7.80 (td, J = 7.5 Hz, J = 1.5 Hz, 1H); 7.72 (t, J = 8.0 Hz, 1H); 7.67 (t, J = 7.5 Hz, 1H); 7.25-7.31 (m, 3H); 4.42 (t, J = 7.5 Hz, 2H); 1.85 (pentet, J = 7.5 Hz, 2H); 1.48 (sextet, J = 7.5 Hz, 2H); 0.98 (t, J = 7.5 Hz, 3H). ESI-MS (CH_3OH): calcd $[M+H]^+$ 383.20; obsd 383.25; calcd $[M+Na]^+$ 405.18; obsd 405.25.

6-Chloro-2,2'-bipyrazine (5): 2,6-Dichloropyrazine (2.42 g, 16.25 mmol), $Pd(PPh_3)_4$ (470 mg, 0.41 mmol) and 2-(tributylstannyl)pyrazine (3.00 g, 8.13 mmol) were dissolved in toluene (150 mL) under nitrogen. The reaction was refluxed for 16 hours. After cooling to room temperature the reaction was quenched with water and the product was extracted with dichloromethane. The organic fraction was dried with $MgSO_4$, filtered and concentrated. Chromatography on silica and eluting with dichloromethane afforded the product in 24% yield (378 mg, 1.96 mmol). The product was used without any further purification. ^{1}H NMR ($CDCl_3$): δ 9.58 (d, J = 1.5 Hz, 1H); 9.51 (s, 1H); 8.67-8.70 (m, 3H). ESI-MS (0.1% Formic Acid in 1:1 CH_3OH:H_2O): calcd $[M+H]^+$ 193.03; obsd 193.00.

***N*-([2,2'-Bipyridin]-6-yl)-*N*-butyl-[2,2'-bipyrazin]-6-amine (L3):** The same procedure as described for **2** was followed using 1,1'-bis(diphenylphosphino)ferrocene (49.0 mg, 0.09 mmol), bis(dibenzylideneacetone)palladium(0) (33.9 mg, 0.06 mmol), *N*-butyl-[2,2'-bipyridin]-6-amine (**1**) (468.4 mg, 2.06 mmol), lithium bis(trimethylsilyl)amide in toluene solution (1 M, 2.75 mL, 2.75 mmol) and 6-chloro-2,2'-bipyrazine (**5**) (378.0 mg, 1.96 mmol). Chromatography on silica and eluting with dichloromethane/20% acetone afforded the product in 65% yield (490 mg, 1.28 mmol). The product was used without any further purification. ^{1}H NMR ($CDCl_3$): δ 9.55 (d, J = 1.5 Hz, 1H); 9.05 (s, 1H); 8.75 (s, 1H); 8.63-8.69 (m, 3H); 8.28 (d, J = 7.5 Hz, 1H); 8.18 (d, J = 8.0 Hz, 1H); 7.84 (t, J = 8.0 Hz, 1H); 7.79 (td, J = 7.5 Hz, J = 2.0 Hz, 1H); 7.31 (ddd, J = 7.5 Hz, J = 5.0 Hz, J = 1.0 Hz, 1H); 7.24 (d, J = 1.0 Hz, 1H); 4.35 (t, J = 7.5 Hz, 2H); 1.85 (pentet, J = 7.5 Hz, 2H); 1.49 (sextet, J =

7.5 Hz, 2H); 0.99 (t, J = 7.5 Hz, 3H). ESI-MS (CH_3OH): calcd $[M+H]^+$ 384.19; obsd 384.25; calcd $[M+Na]^+$ 406.18; obsd 406.25.

6-Bromo-*N*-(6-bromopyridin-2-yl)-*N*-butylpyridin-2-amine (6): The same procedure as described for **4** was followed using XantPhos (197.7 mg, 0.34 mmol), tris(dibenzylideneacetone)dipalladium(0) (156.5 mg, 0.17 mmol), *n*-butylamine (500 mg, 6.84 mmol), potassium tert-butoxide (2.30 g, 20.51 mmol) and 2,6-dibromopyridine (4.86 g, 20.59 mmol). Chromatography on silica and eluting with dichloromethane/hexanes (1:2 ratio) afforded the product in 39% yield (1.31 g, 3.40 mmol). The product was used without any further purification. ^1H NMR ($CDCl_3$): δ 7.37 (t, J = 8.0 Hz, 2H); 7.08 (d, J = 8.0, 2H); 7.04 (d, J = 7.5 Hz, 2H); 4.14 (t, J = 7.5 Hz, 2H); 1.66 (pentet, J = 7.5 Hz, 2H); 1.36 (sextet, J = 7.5 Hz, 2H); 0.94 (t, J = 7.5 Hz, 3H). ESI-MS (CH_3OH): calcd $[M+H]^+$ 385.97; obsd 386.00; calcd $[M+Na]^+$ 407.95; obsd 408.00.

***N*-Butyl-6-(pyrazin-2-yl)-*N*-(6-(pyrazin-2-yl)pyridin-2-yl)pyridin-2-amine (L4):** 6-Bromo-*N*-(6-bromopyridin-2-yl)-*N*-butylpyridin-2-amine (**6**) (434.7 mg, 1.13 mmol), $Pd(PPh_3)_4$ (60.3 mg, 0.05 mmol) and 2-(tributylstannyl)pyrazine (1.00 g, 2.71 mmol) were dissolved in toluene (30 mL) under nitrogen. The reaction was refluxed for 16 hours. After cooling to room temperature the reaction was quenched with water and the product was extracted with dichloromethane. The organic fraction was dried with $MgSO_4$, filtered and concentrated. Chromatography on silica and eluting with dichloromethane/20% acetone afforded the product in 40% yield (174 mg, 0.45 mmol). The product was used without any further purification. ^1H NMR ($CDCl_3$): δ 9.58 (d, J = 1.5 Hz, 2H); 8.57-8.62 (m, 4H); 7.98 (dd, J = 7.5 Hz, J = 0.5 Hz, 2H); 7.72 (t, J = 7.5 Hz, 2H); 7.30 (d, J = 8.0 Hz, 2H); 4.41 (t, J = 7.5 Hz, 2H); 1.87 (pentet, J = 7.5 Hz, 2H); 1.49 (sextet, J = 7.5 Hz, 2H); 0.99 (t, J = 7.5 Hz, 3H). ESI-MS (CH_3OH): calcd $[M+H]^+$ 384.19; obsd 384.25; calcd $[M+Na]^+$ 406.18; obsd 406.25.

$[Co(L1)(CH_3CN)](ClO_4)_2$: $Co(ClO_4)_2{\cdot}6H_2O$ (32.9 mg, 0.090 mmol) and **L1** (34.4 mg, 0.090 mmol) were dissolved in acetonitrile (5 mL). After the reaction mixture was heated to reflux the solution was allowed to cool to room temperature. Diethyl ether was allowed to diffuse into the acetonitrile solution. The crystals were filtered and washed with diethyl ether. The product was obtained as dark yellow/green crystals in 73% yield (45 mg). ESI-MS (CH_3CN): calcd $[M]^{2+}$ 220.56; obsd 220.58; calcd $[M+ClO_4]^+$ 540.07; obsd 540.00. Anal. calcd. for **$[Co(L1)(CH_3CN)](ClO_4)_2$**, $C_{25}H_{25}Cl_2CoN_7O_8{\cdot}1/4H_2O$: C, 43.78; H, 3.75; N, 14.30. Found: C, 43.78; H, 3.65; N, 13.94.

$[Co(L2)(CH_3CN)](ClO_4)_2$: The same procedure as described for **$[Co(L1)(CH_3CN)](ClO_4)_2$** was followed using $Co(ClO_4)_2{\cdot}6H_2O$ (28.0 mg, 0.077 mmol) and **L2** (29.3 mg, 0.077 mmol). The product was obtained as dark yellow/green crystals in 77% yield (40 mg). ESI-MS (CH_3CN): calcd $[M]^{2+}$ 220.56; obsd 220.58; calcd $[M+ClO_4]^+$ 540.07; obsd 540.00. Anal. calcd. for **$[Co(L2)(CH_3CN)](ClO_4)_2$**, $C_{25}H_{25}Cl_2CoN_7O_8{\cdot}1/4(CH_3CH_2)_2O{\cdot}1/2CH_3CN$: C, 45.02; H, 4.06; N, 14.58. Found: C, 45.35; H, 3.75; N, 14.87.

$[Co(L3)(CH_3CN)](ClO_4)_2$: The same procedure as described for **$[Co(L1)(CH_3CN)](ClO_4)_2$** was followed using $Co(ClO_4)_2{\cdot}6H_2O$ (54.2 mg, 0.148 mmol) and **L3** (56.8 mg, 0.148 mmol). The product was obtained as dark yellow/green crystals in 90% yield (91 mg). ESI-MS (CH_3CN): calcd $[M]^{2+}$ 221.06; obsd 221.00; calcd $[M+ClO_4]^+$ 541.07; obsd 541.00. Anal. calcd. for **$[Co(L3)(CH_3CN)](ClO_4)_2$**, $C_{24}H_{24}Cl_2CoN_8O_8$: C, 42.25; H, 3.55; N, 16.42. Found: C, 42.26; H, 3.50; N, 16.40.

$[Co(L4)(CH_3CN)](ClO_4)_2$: The same procedure as described for **$[Co(L1)(CH_3CN)](ClO_4)_2$** was followed using $Co(ClO_4)_2{\cdot}6H_2O$ (44.7 mg, 0.122 mmol) and **L4** (46.8 mg, 0.122 mmol). The product was obtained as dark yellow/green crystals in 61% yield (51 mg). ESI-MS (CH_3CN): calcd $[M]^{2+}$ 221.06; obsd 221.00; calcd $[M+ClO_4]^+$ 541.07; obsd 541.00. Anal. calcd. for **$[Co(L4)(H_2O)_2](ClO_4)_2$**, $C_{22}H_{25}Cl_2CoN_7O_{10}$: C, 39.01; H, 3.72; N, 14.48. Found: C, 39.17; H, 3.63; N, 14.58.

^{1}H NMR spectra of intermediates and ligands

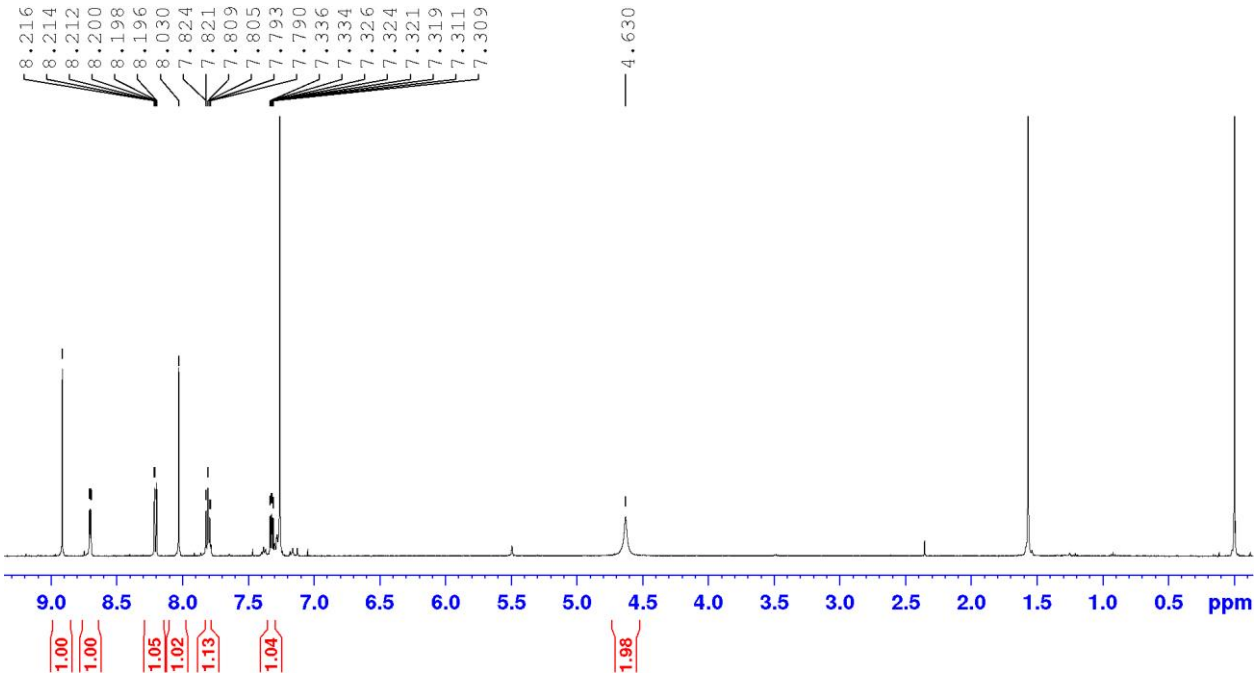

Figure S1. ^{1}H NMR spectrum of **6-(pyridin-2-yl)pyrazin-2-amine** (**1**) in $CDCl_3$.

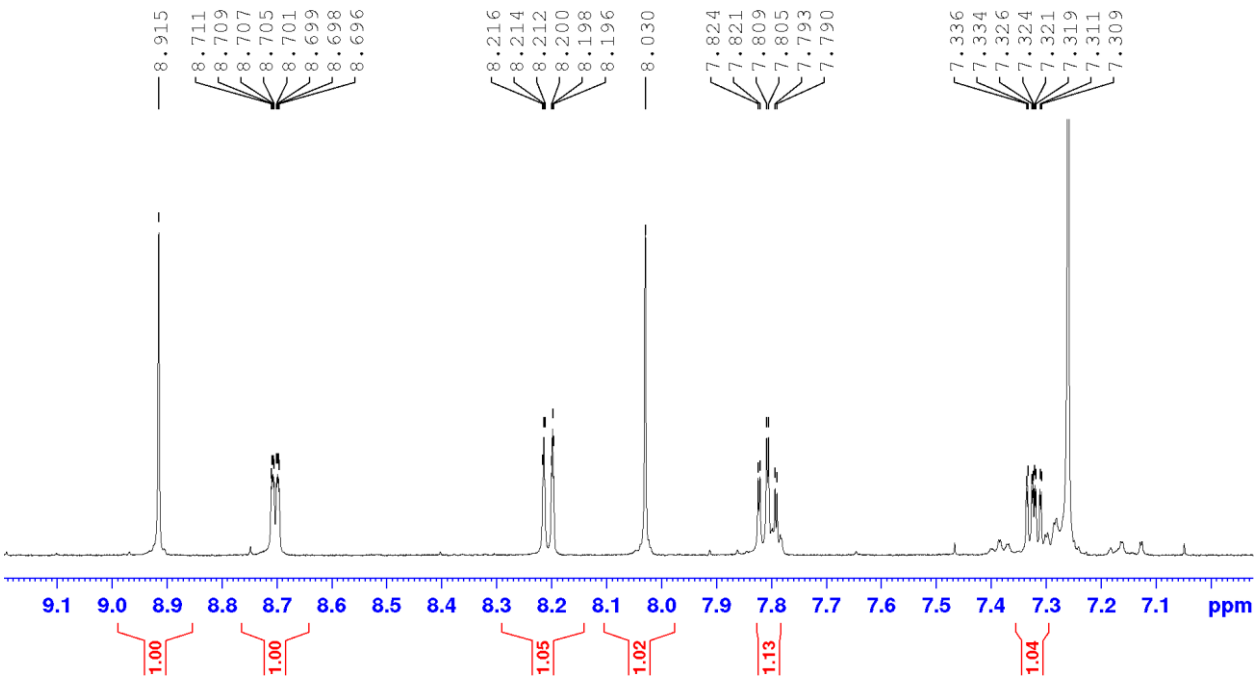

Figure S2. Aromatic region of ^{1}H NMR spectrum of **6-(pyridin-2-yl)pyrazin-2-amine** (**1**) in $CDCl_3$.

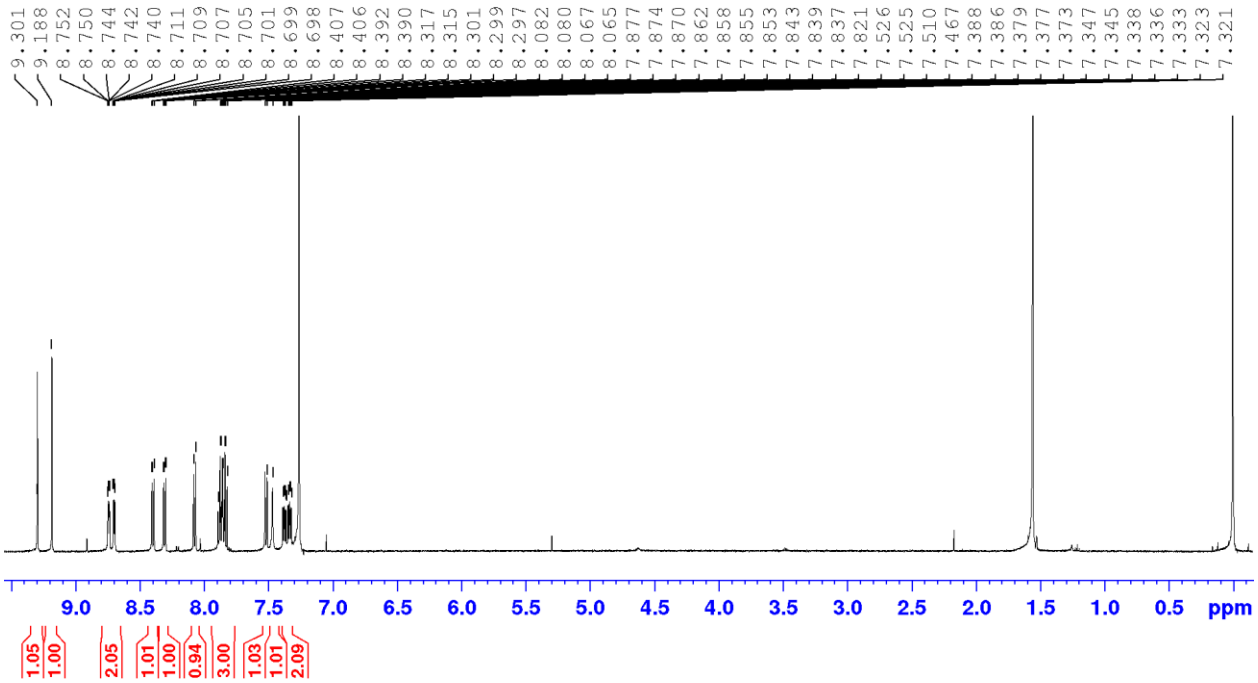

Figure S3. ^{1}H NMR spectrum of ***N*-(6-(pyridin-2-yl)pyrazin-2-yl)-[2,2'-bipyridin]-6-amine** (**2**) in $CDCl_3$.

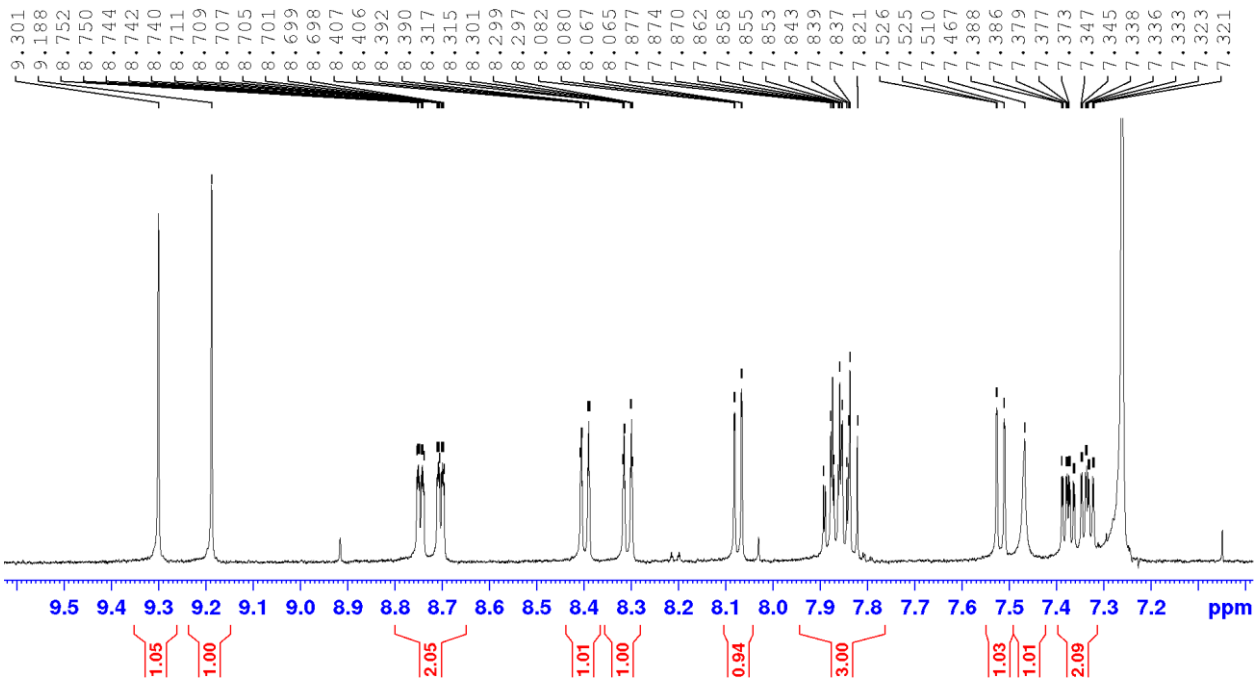

Figure S4. Aromatic region of ^{1}H NMR spectrum of ***N*-(6-(pyridin-2-yl)pyrazin-2-yl)-[2,2'-bipyridin]-6-amine** (**2**) in $CDCl_3$.

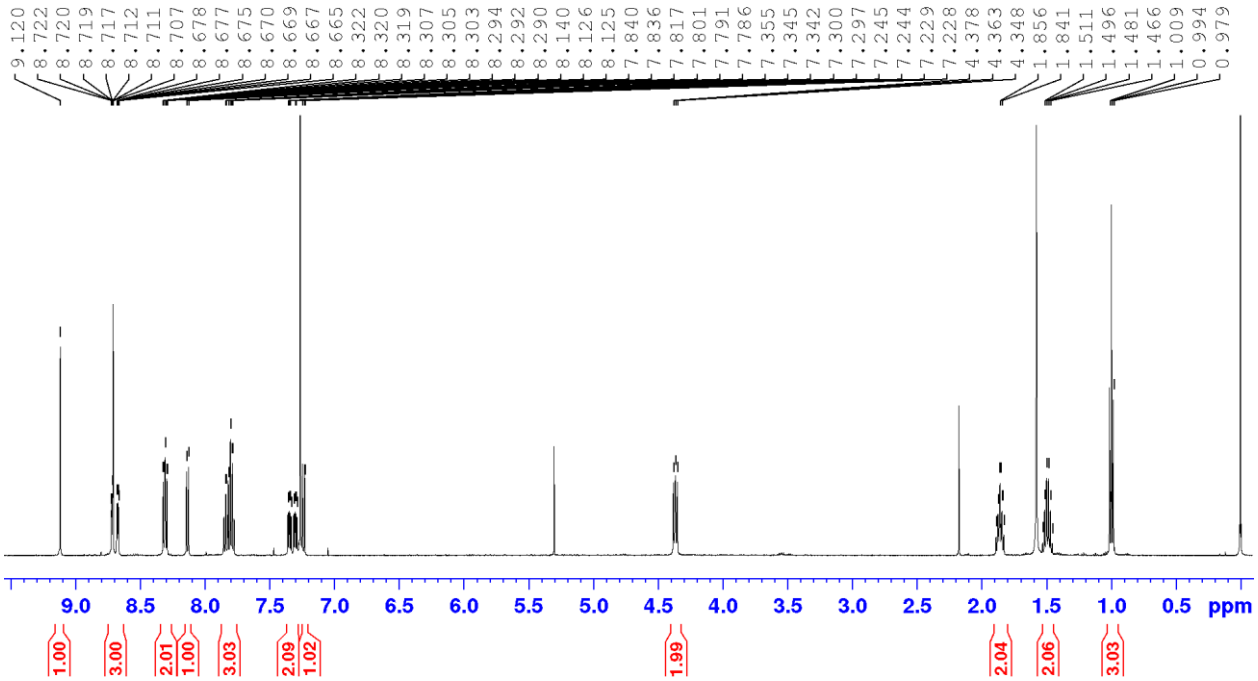

Figure S5. ^{1}H NMR spectrum of ***N*-butyl-*N*-(6-(pyridin-2-yl)pyrazin-2-yl)-[2,2'-bipyridin]-6-amine** (**L1**) in $CDCl_3$.

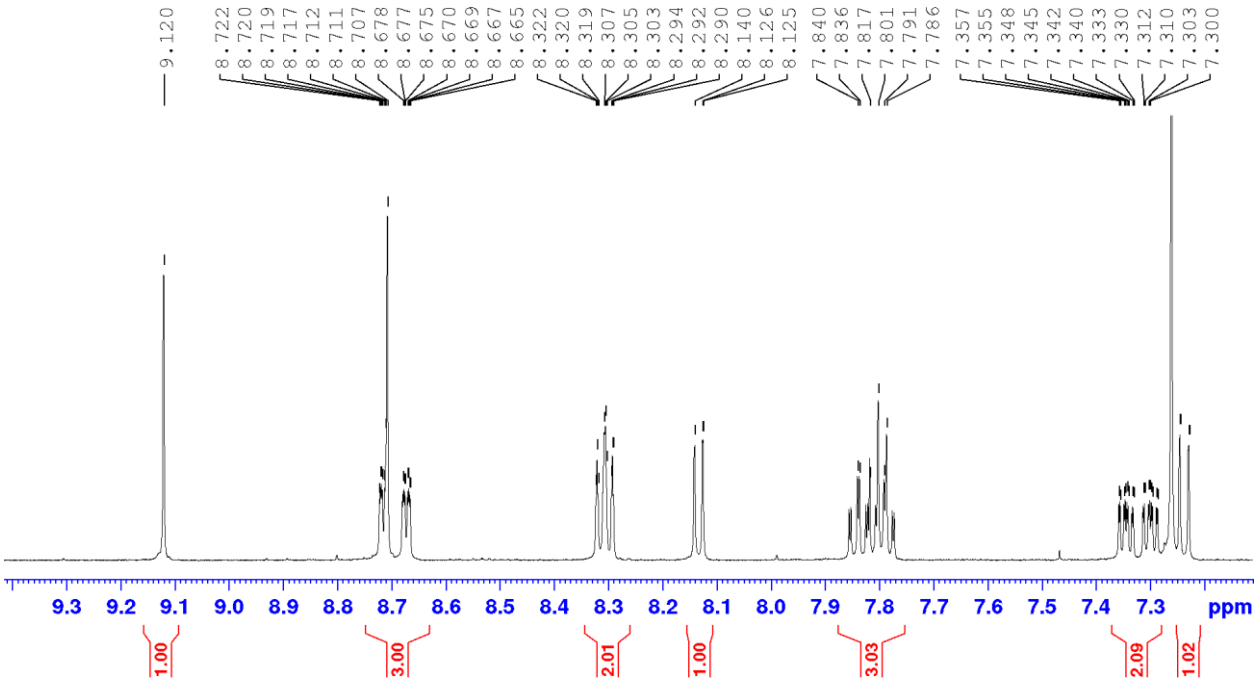

Figure S6. Aromatic region of ^{1}H NMR spectrum of ***N*-butyl-*N*-(6-(pyridin-2-yl)pyrazin-2-yl)-[2,2'-bipyridin]-6-amine** (**L1**) in $CDCl_3$.

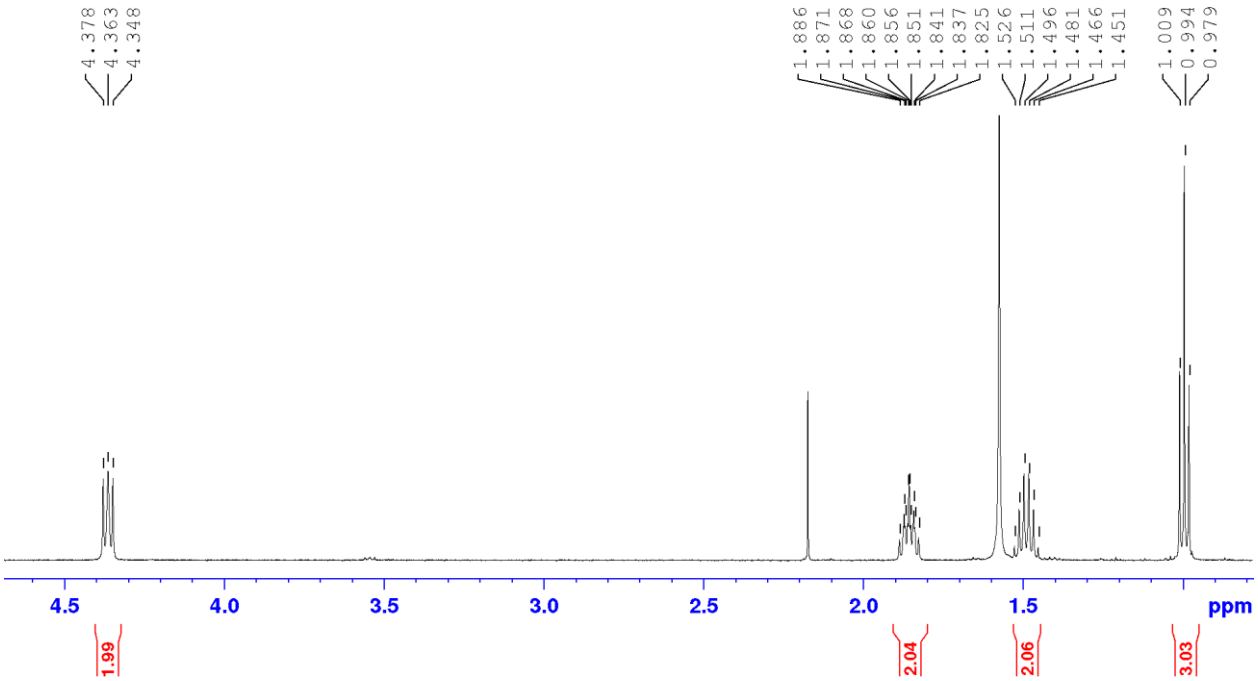

Figure S7. Aliphatic region of ^{1}H NMR spectrum of ***N*-butyl-*N*-(6-(pyridin-2-yl)pyrazin-2-yl)-[2,2'-bipyridin]-6-amine** (**L1**) in $CDCl_3$.

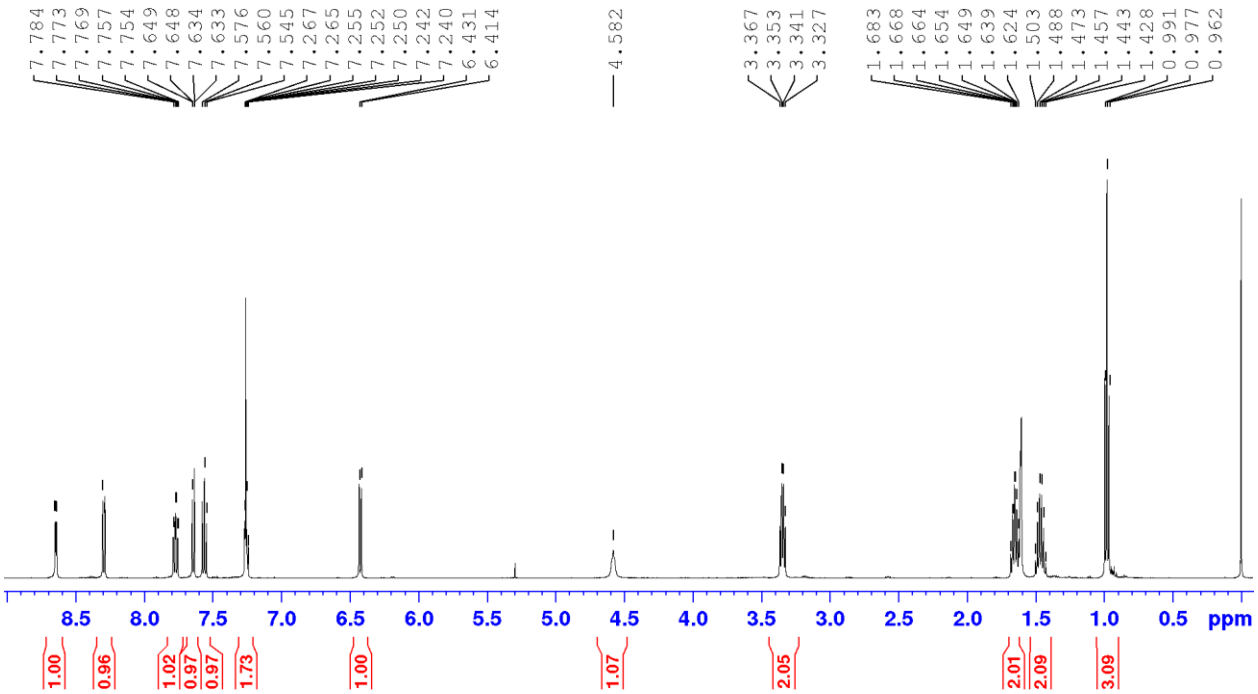

Figure S8. ^{1}H NMR spectrum of ***N*-butyl-[2,2'-bipyridin]-6-amine** (**3**) in $CDCl_3$.

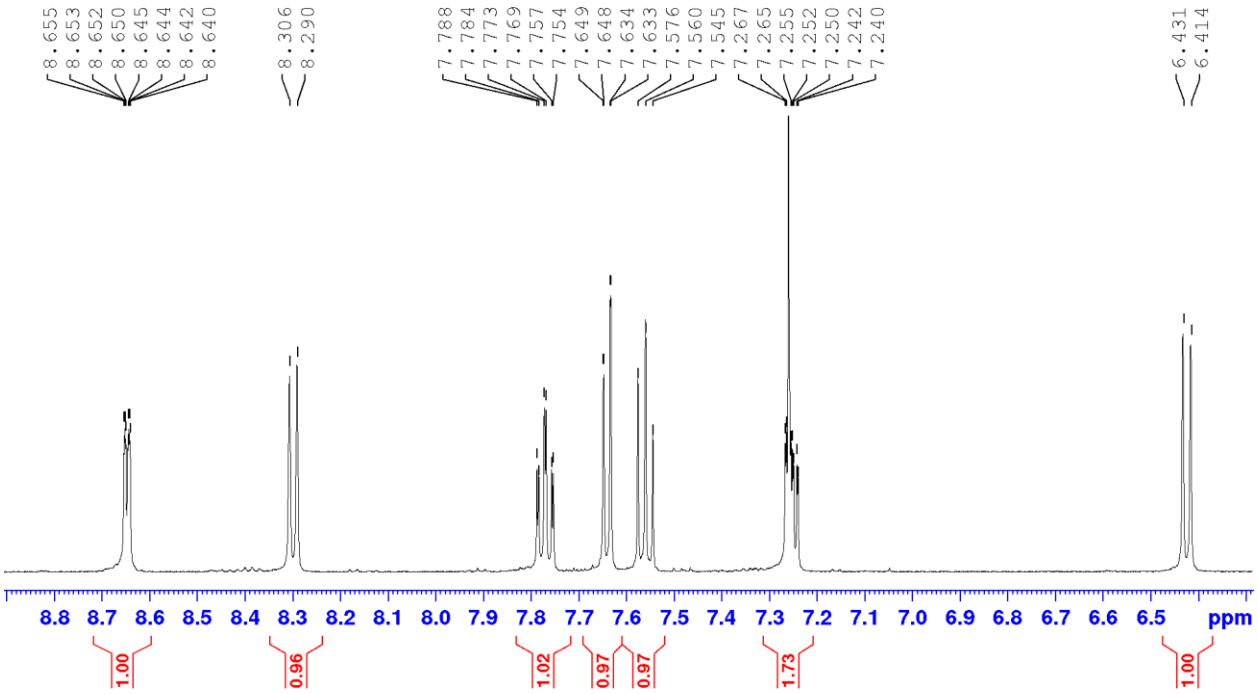

Figure S9. Aromatic region of ^{1}H NMR spectrum of ***N*-butyl-[2,2'-bipyridin]-6-amine** (**3**) in $CDCl_3$.

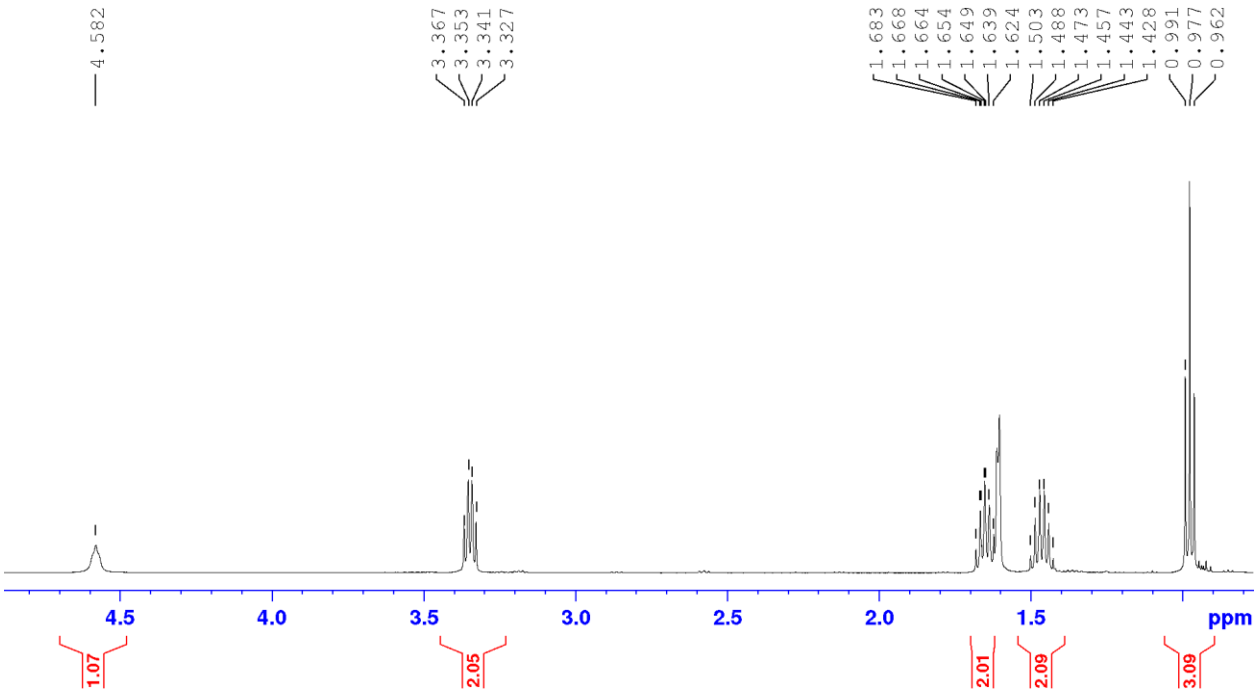

Figure S10. Aliphatic region of ^{1}H NMR spectrum of ***N*-butyl-[2,2'-bipyridin]-6-amine** (**3**) in $CDCl_3$.

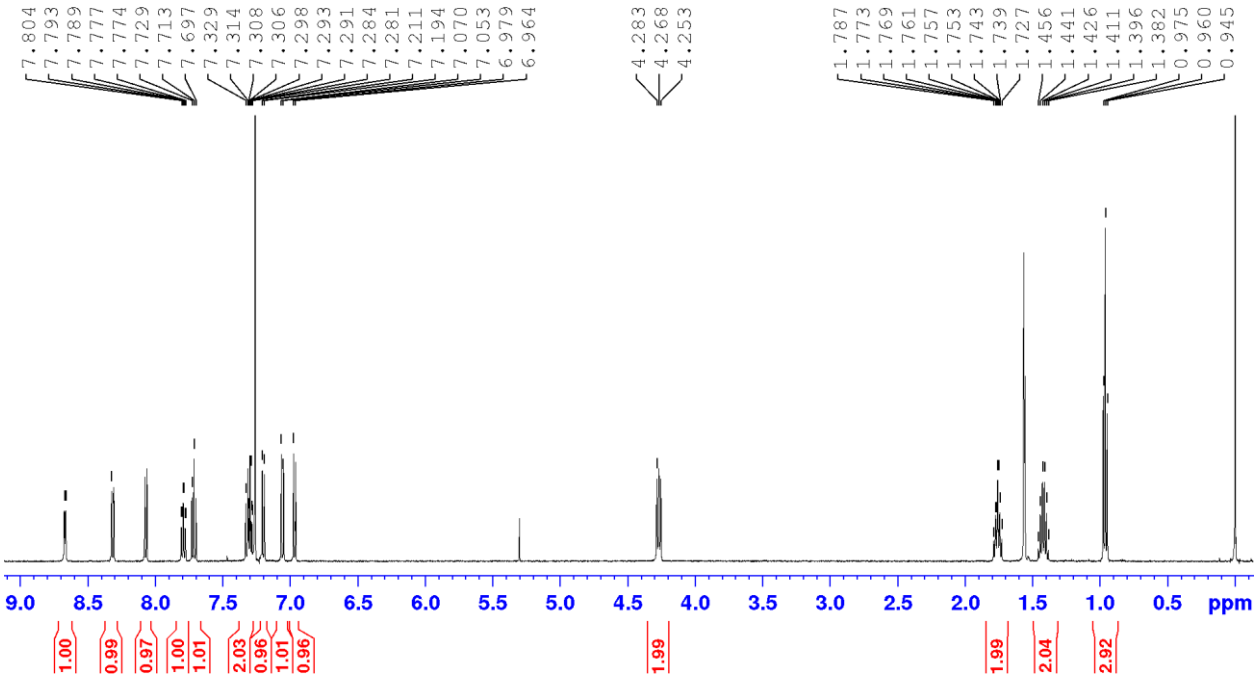

Figure S11. [1]H NMR spectrum of ***N*-(6-bromopyridin-2-yl)-*N*-butyl-[2,2'-bipyridin]-6-amine** (**4**) in $CDCl_3$.

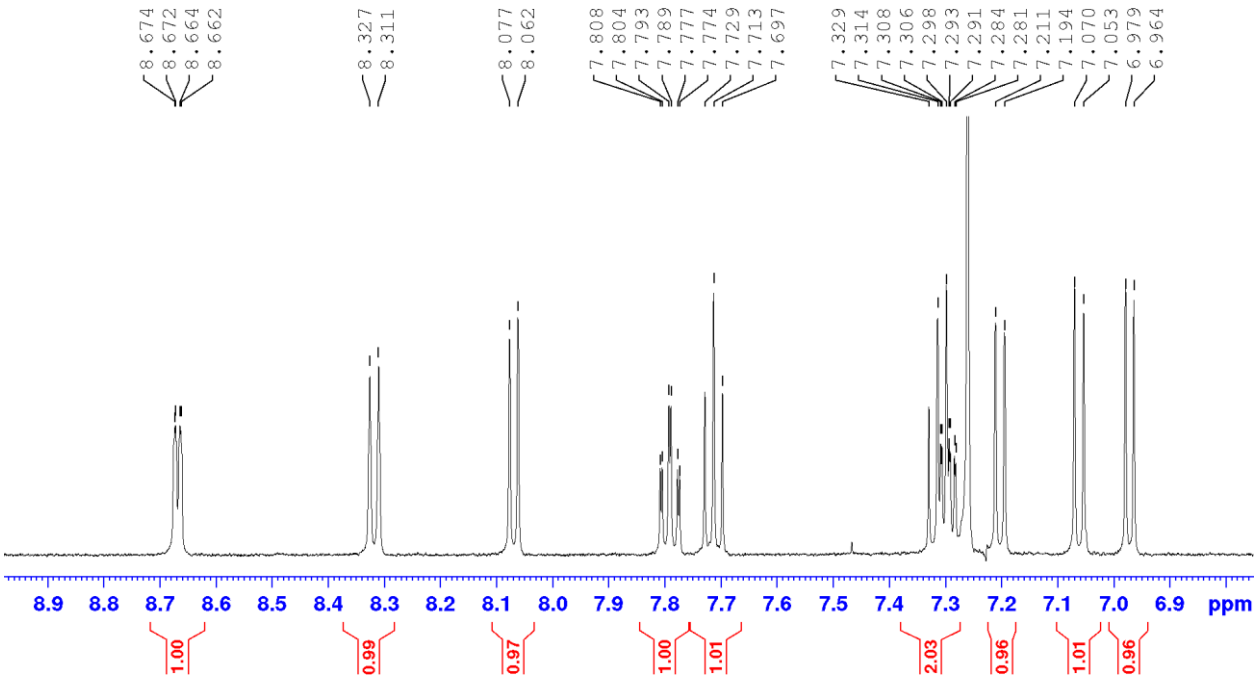

Figure S12. Aromatic region of [1]H NMR spectrum of ***N*-(6-bromopyridin-2-yl)-*N*-butyl-[2,2′-bipyridin]-6-amine** (**4**) in $CDCl_3$.

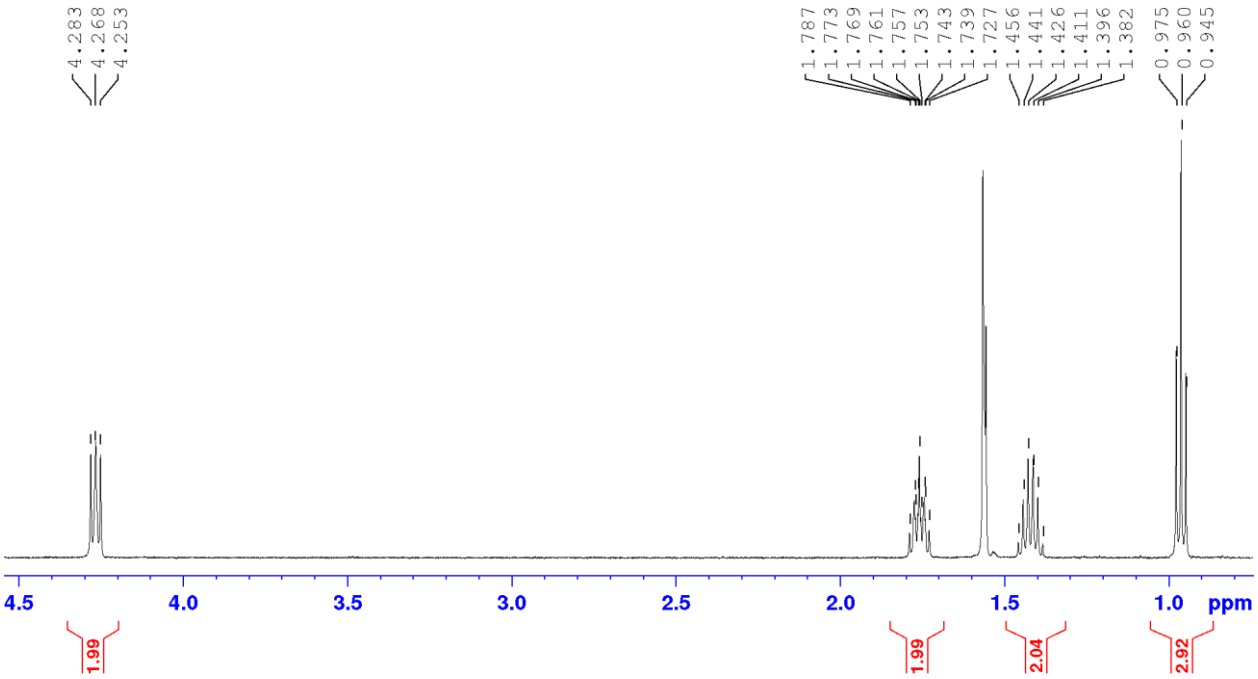

Figure S13. Aliphatic region of ^{1}H NMR spectrum of ***N*-(6-bromopyridin-2-yl)-*N*-butyl-[2,2′ -bipyridin]-6-amine** (**4**) in $CDCl_3$.

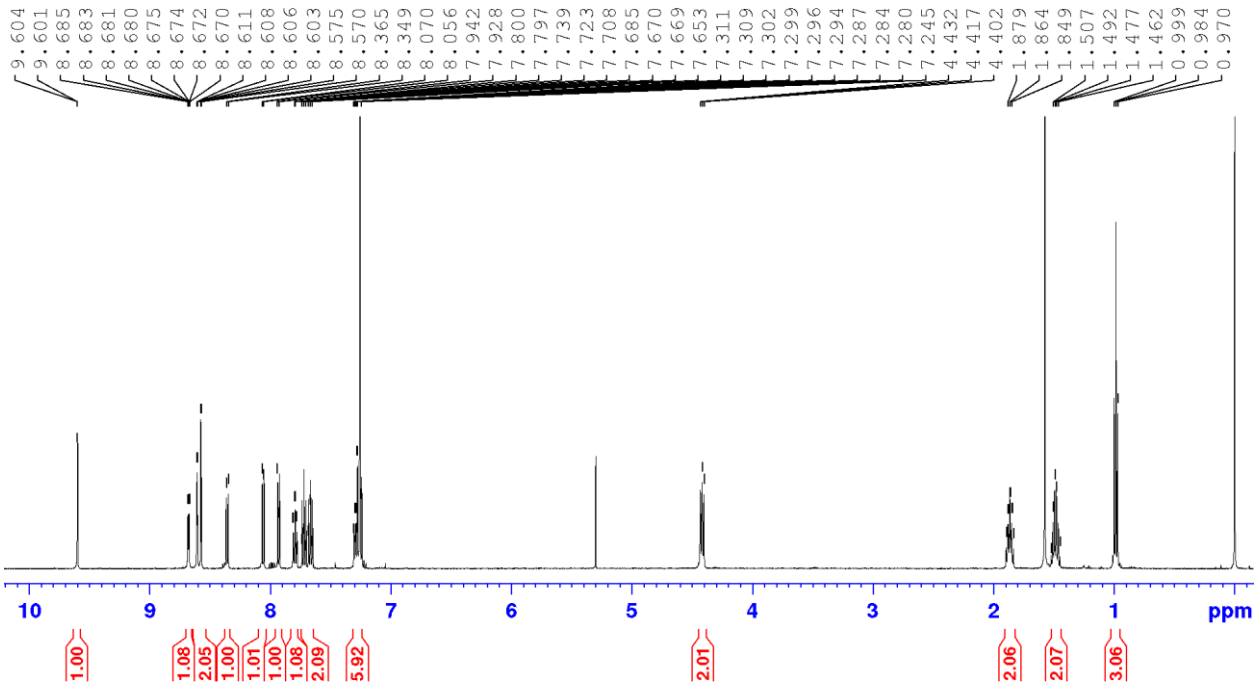

Figure S14. ^{1}H NMR spectrum of ***N*-butyl-*N*-(6-(pyrazin-2-yl)pyridin-2-yl)-[2,2'-bipyridin]-6-amine** (**L2**) in $CDCl_3$.

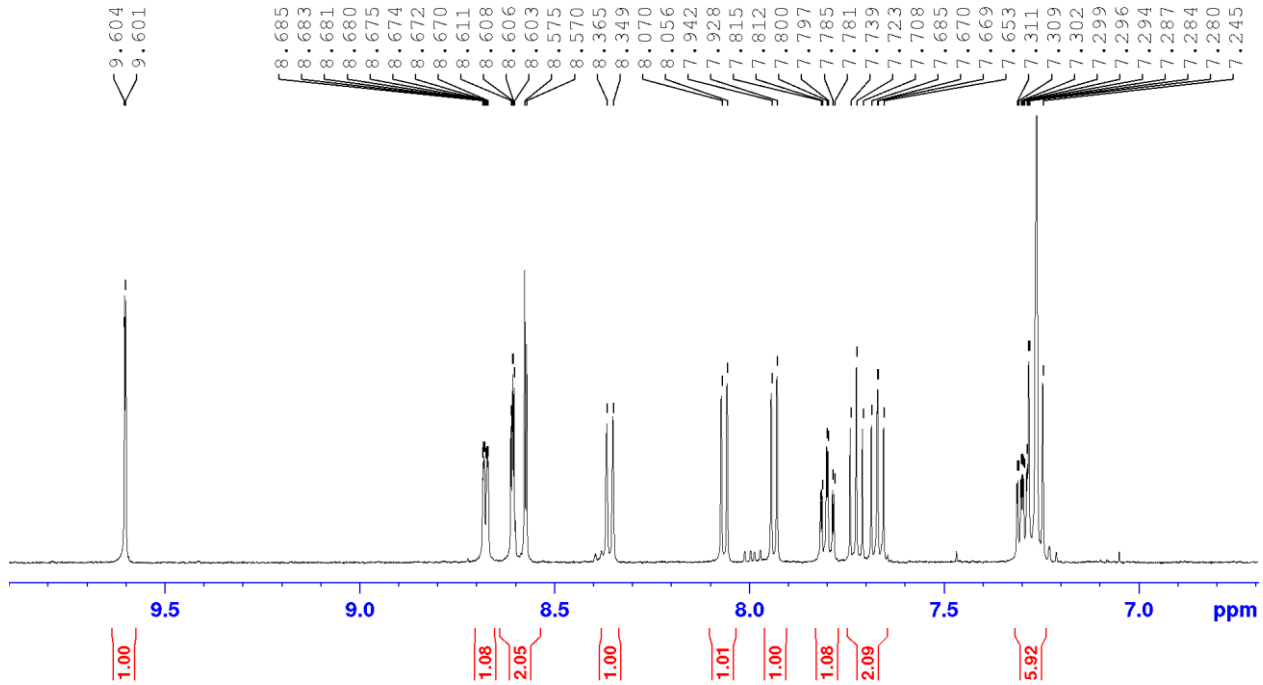

Figure S15. Aromatic region of ^{1}H NMR spectrum of ***N*-butyl-*N*-(6-(pyrazin-2-yl)pyridin-2-yl)-[2,2'-bipyridin]-6-amine** (**L2**) in $CDCl_3$.

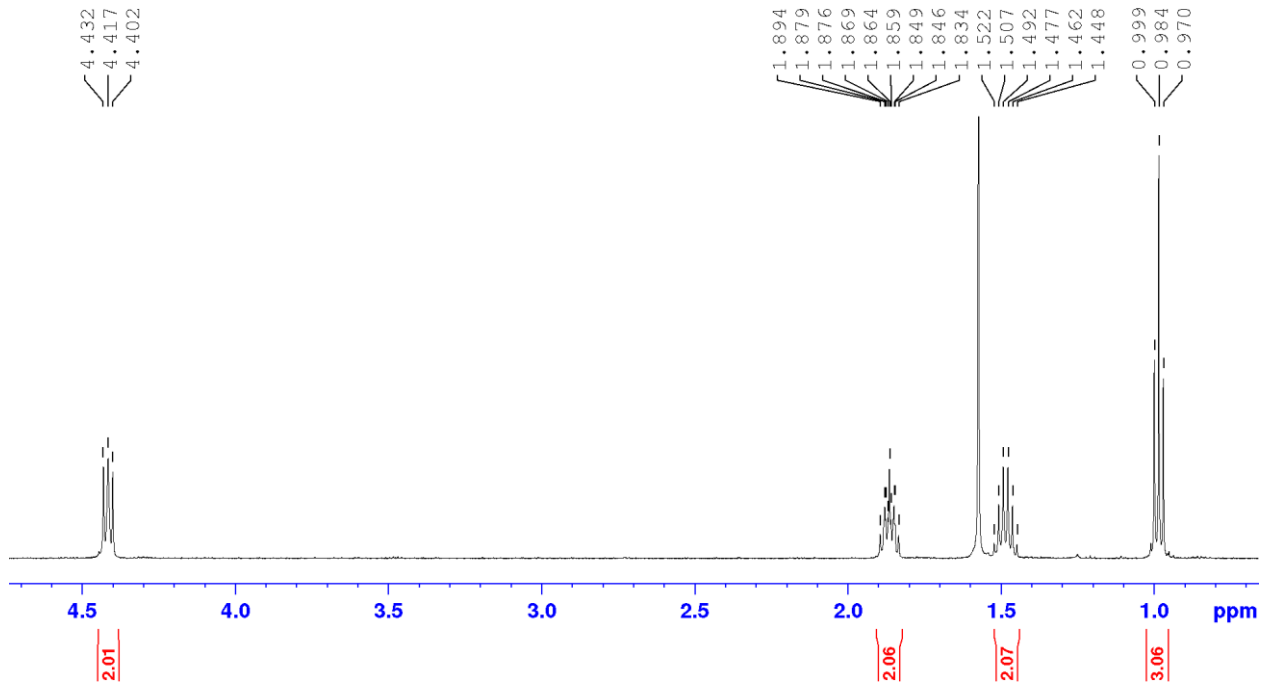

Figure S16. Aliphatic region of ^{1}H NMR spectrum of ***N*-butyl-*N*-(6-(pyrazin-2-yl)pyridin-2-yl)-[2,2'-bipyridin]-6-amine** (**L2**) in $CDCl_3$.

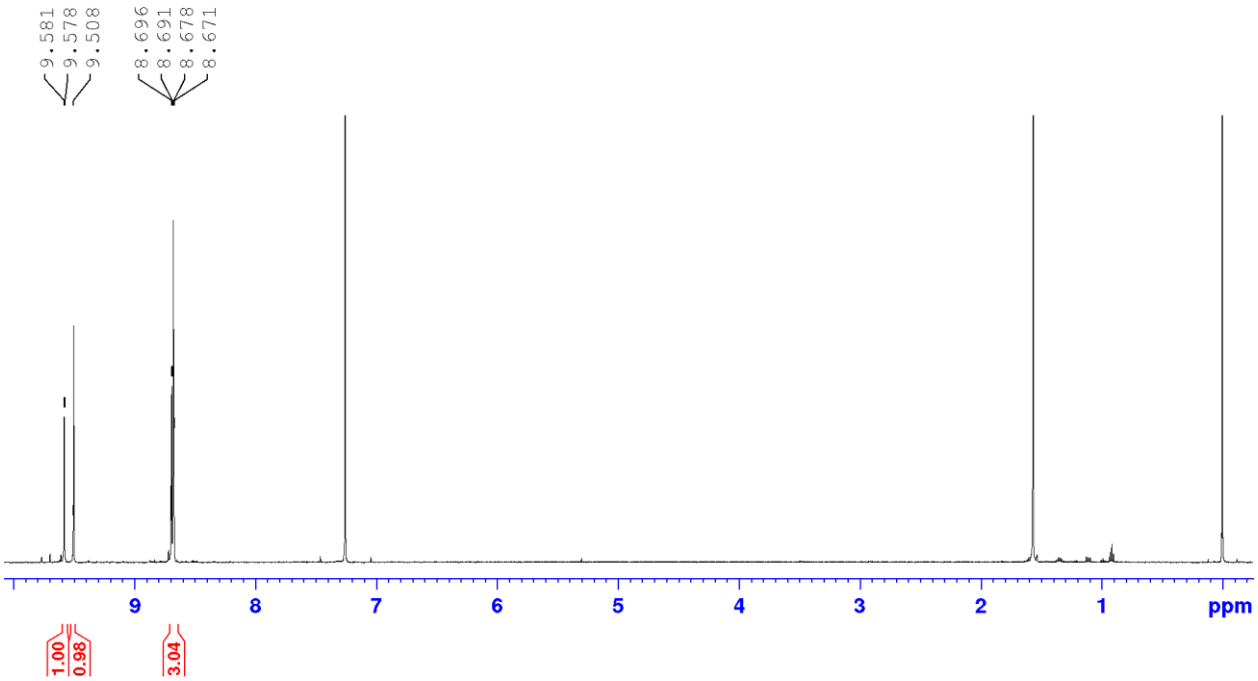

Figure S17. ^{1}H NMR spectrum of **6-chloro-2,2'-bipyrazine** (**5**) in $CDCl_3$.

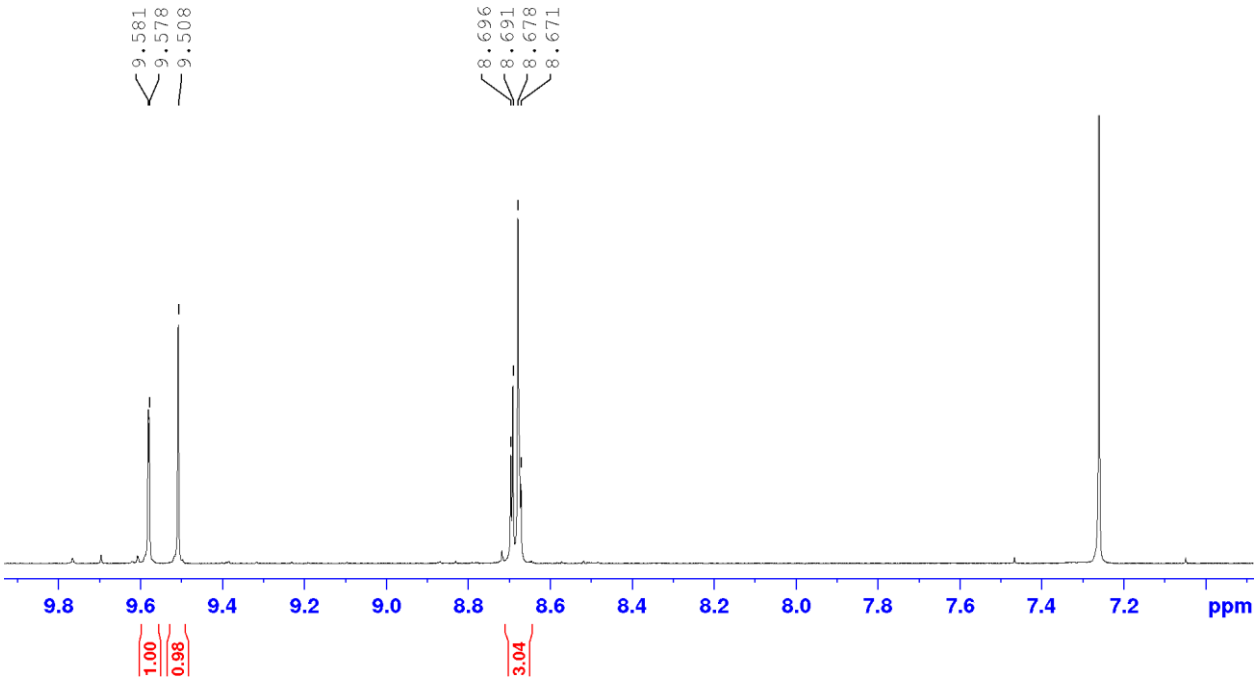

Figure S18. Aromatic region of ^{1}H NMR spectrum of **6-chloro-2,2'-bipyrazine** (**5**) in $CDCl_3$.

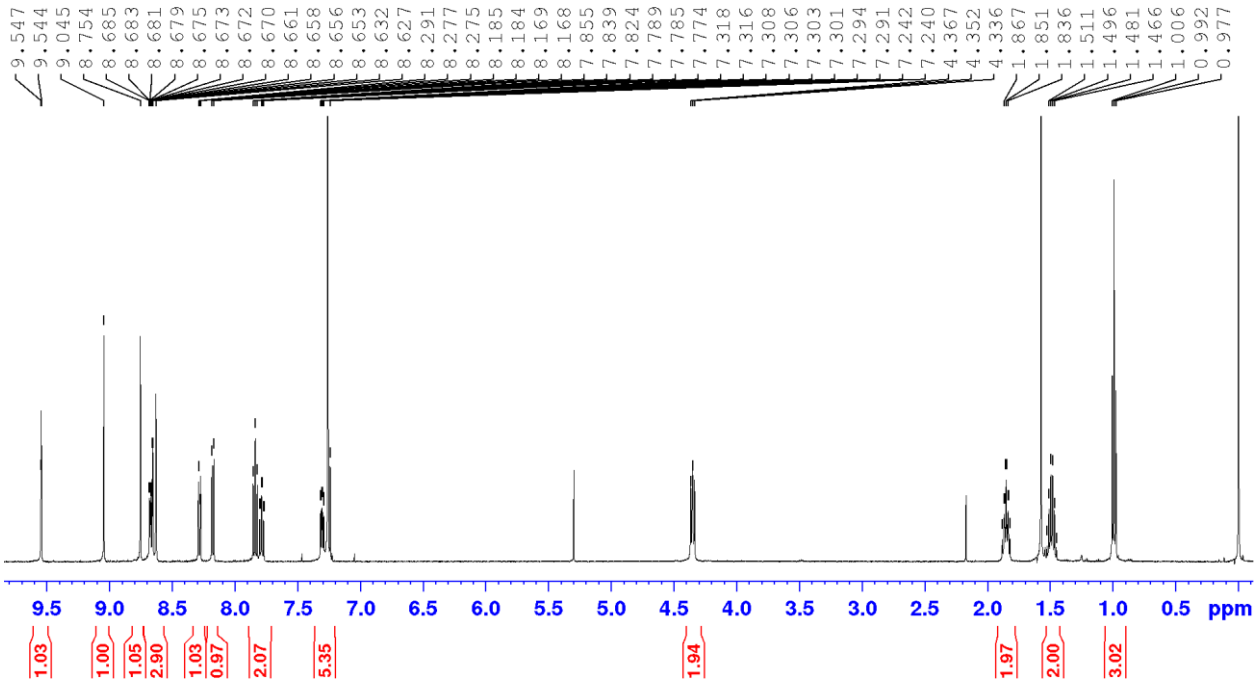

Figure S19. ^{1}H NMR spectrum of ***N*-([2,2'-bipyridin]-6-yl)-*N*-butyl-[2,2'-bipyrazin]-6-amine** (**L3**) in $CDCl_3$.

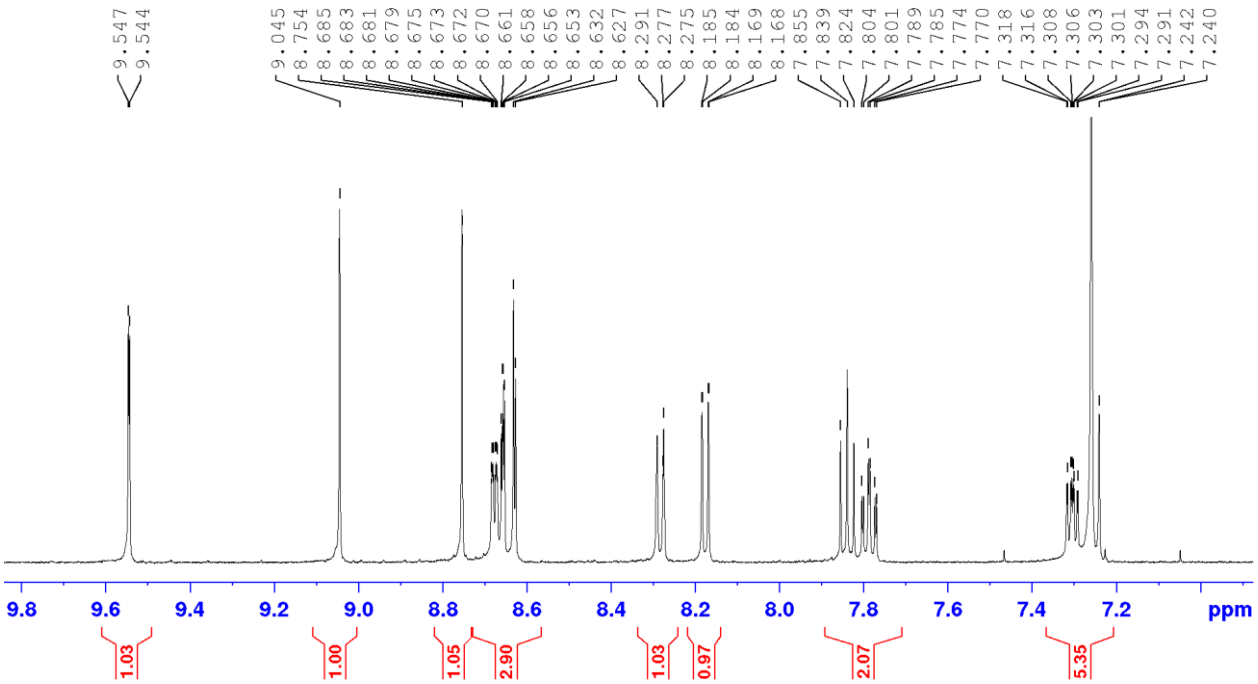

Figure S20. Aromatic region of ^{1}H NMR spectrum of ***N*-([2,2'-bipyridin]-6-yl)-*N*-butyl-[2,2'-bipyrazin]-6-amine** (**L3**) in $CDCl_3$.

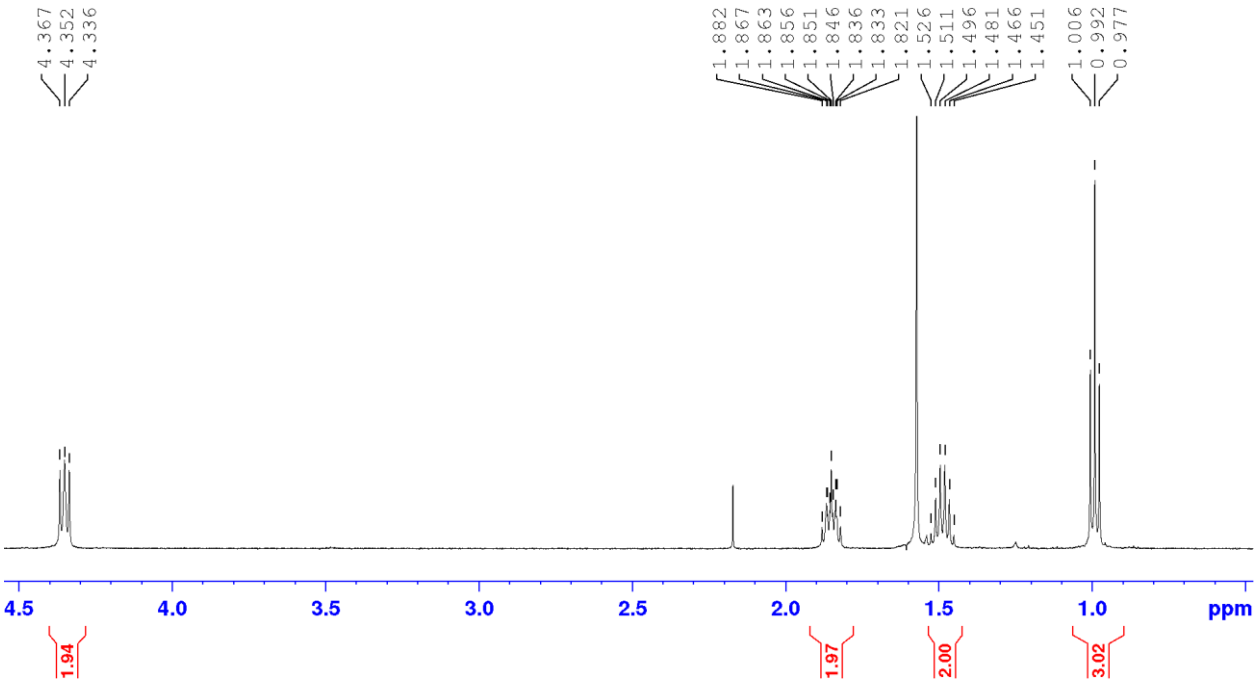

Figure S21. Aliphatic region of ^{1}H NMR spectrum of ***N*-([2,2'-bipyridin]-6-yl)-*N*-butyl-[2,2'-bipyrazin]-6-amine** (**L3**) in $CDCl_3$.

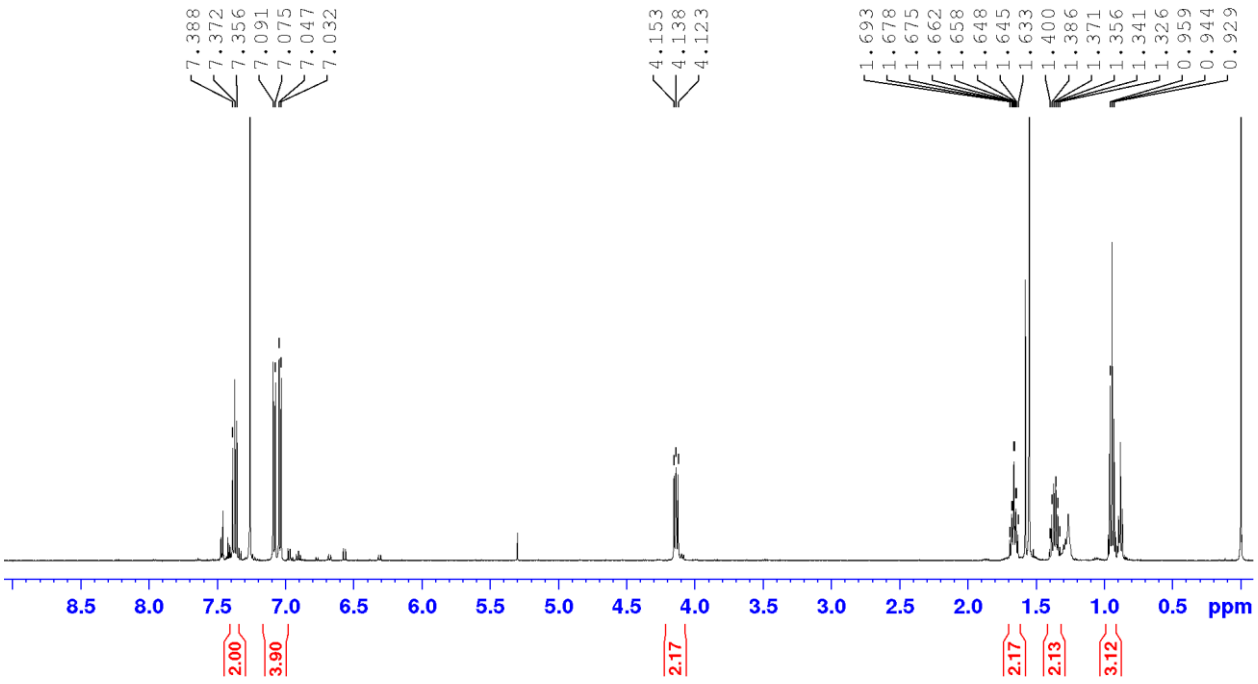

Figure S22. ^{1}H NMR spectrum of **6-Bromo-*N*-(6-bromopyridin-2-yl)-*N*-butylpyridin-2-amine** (**6**) in $CDCl_3$.

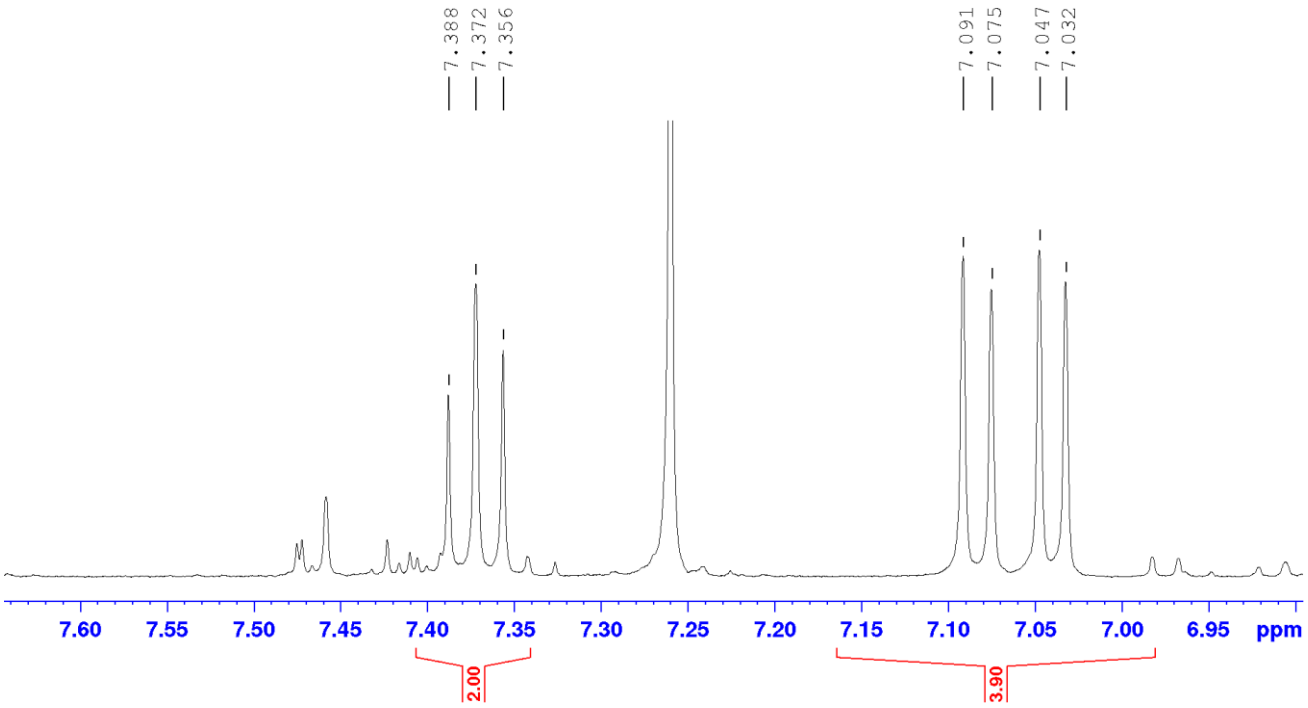

Figure S23. Aromatic region of ^{1}H NMR spectrum of **6-Bromo-*N*-(6-bromopyridin-2-yl)-*N*-butylpyridin-2-amine** (**6**) in $CDCl_3$.

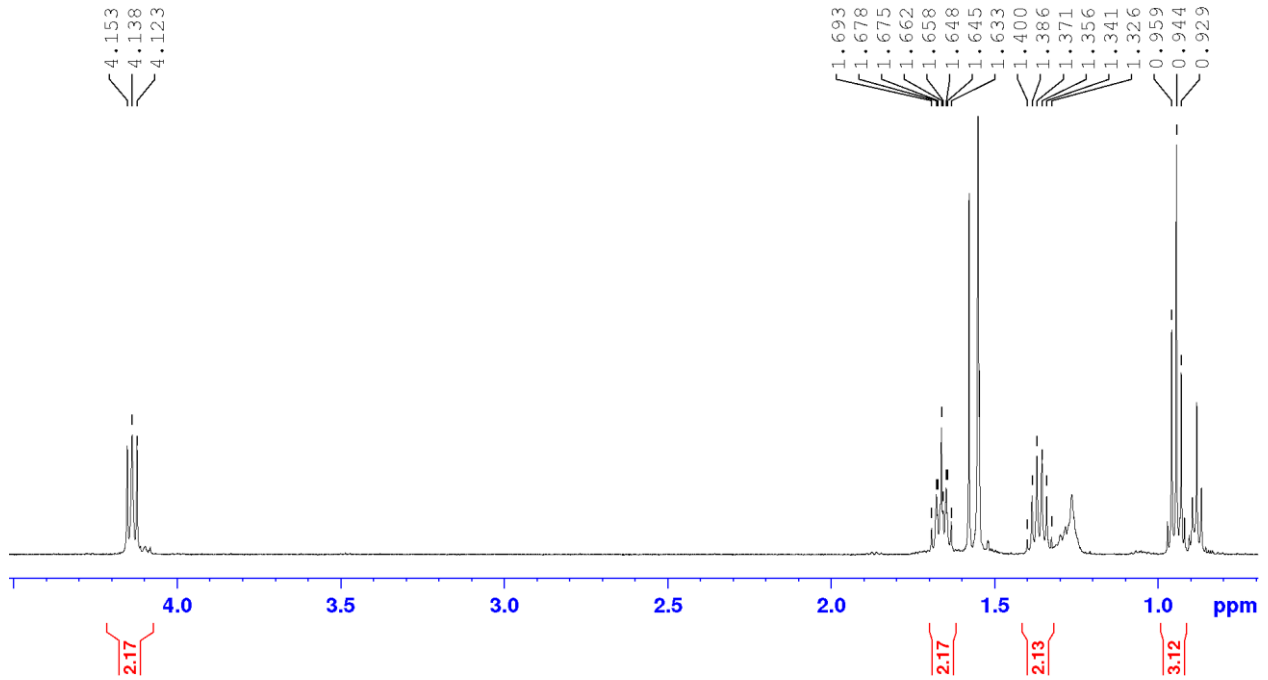

Figure S24. Aliphatic region of ^{1}H NMR spectrum of **6-Bromo-*N*-(6-bromopyridin-2-yl)-*N*-butylpyridin-2-amine** (**6**) in $CDCl_3$.

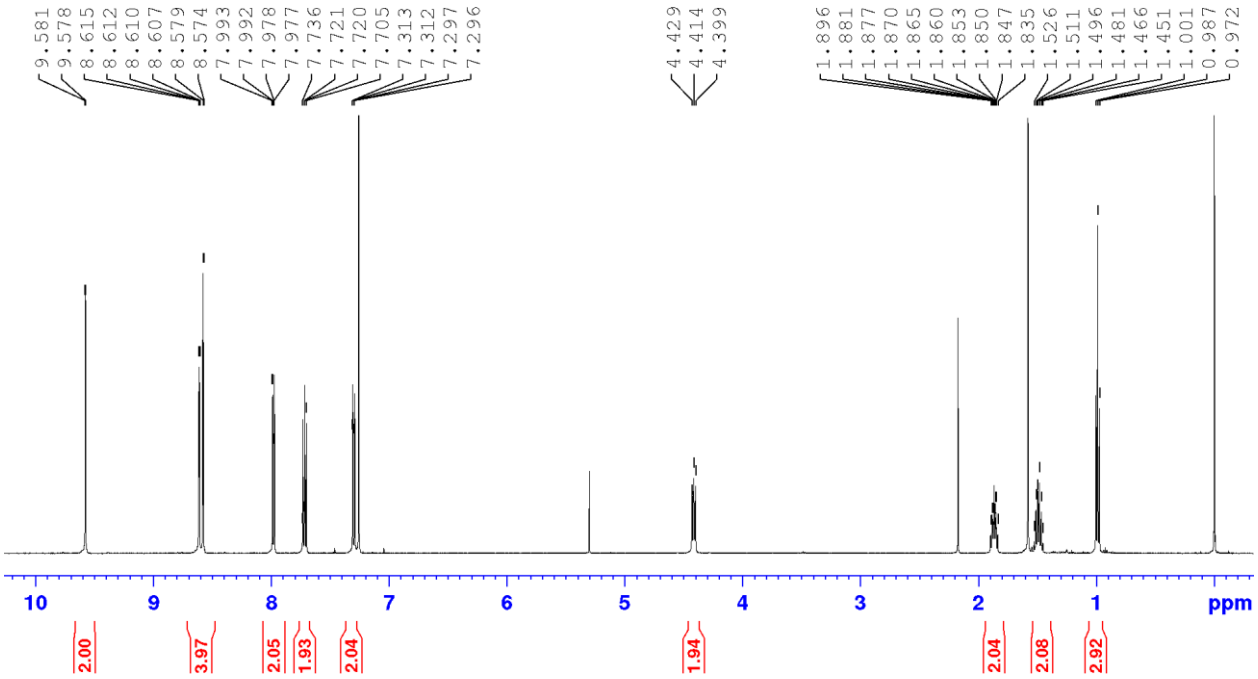

Figure S25. ^{1}H NMR spectrum of ***N*-butyl-6-(pyrazin-2-yl)-*N*-(6-(pyrazin-2-yl)pyridin-2-yl)pyridin-2-amine** (**L4**) in $CDCl_3$.

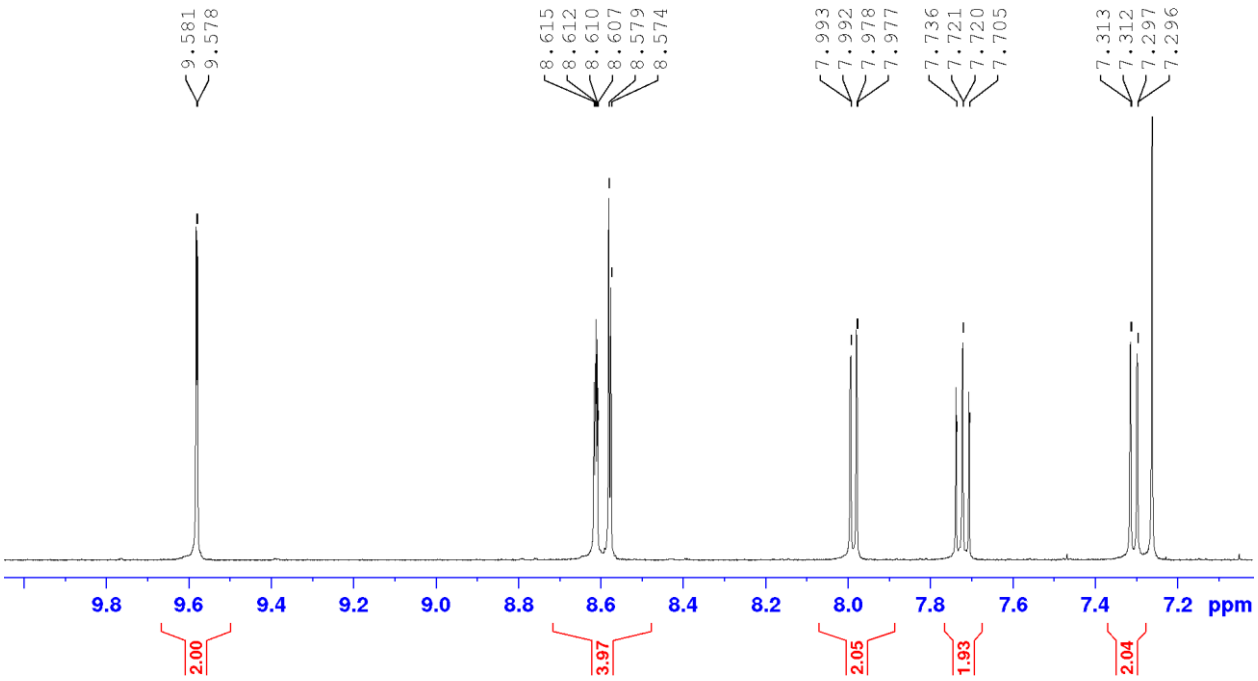

Figure S26. Aromatic region of ^{1}H NMR spectrum of ***N*-butyl-6-(pyrazin-2-yl)-*N*-(6-(pyrazin-2-yl)pyridin-2-yl)pyridin-2-amine** (**L4**) in $CDCl_3$.

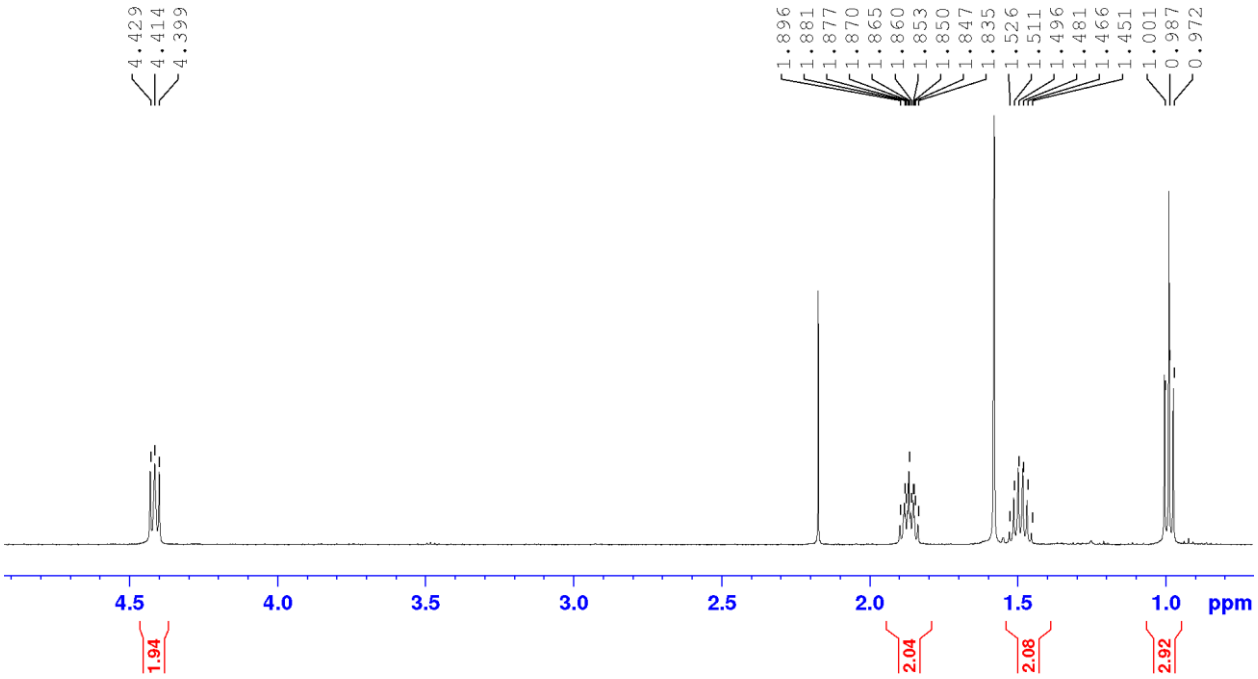

Figure S27. Aliphatic region of ^{1}H NMR spectrum of ***N*-butyl-6-(pyrazin-2-yl)-*N*-(6-(pyrazin-2-yl)pyridin-2-yl)pyridin-2-amine** (**L4**) in $CDCl_3$.

Crystal structure data

Single crystals of **1-4** were coated with a trace of Fomblin oil and quickly transferred to the goniometer head of a Bruker Quest diffractometer with a fixed chi angle, a sealed tube fine focus X-ray source, single crystal curved graphite incident beam monochromator, a Photon100 CMOS area detector and an Oxford Cryosystems low temperature device. Examination and data collection were performed with Mo Kα radiation (λ = 0.71073 Å) at 150 K. Data were collected, reflections were indexed and processed, and the files scaled and corrected for absorption using APEX3[1] and SADABS.[2]

The space groups were assigned using XPREP within the SHELXTL suite of programs and the structures were solved by direct methods using ShelXS[3] and refined by full matrix least squares against F^2 with all reflections with Shelxl2018[4] using the graphical interface ShelXle.[5] H atoms were positioned geometrically and constrained to ride on their parent atoms, with carbon hydrogen bond distances of 0.95 Å for aromatic C-H, and 0.99 and 0.98 Å for aliphatic CH_2 and CH_3 moieties, respectively. Methyl H atoms were allowed to rotate but not to tip to best fit the experimental electron density. U_{iso}(H) values were set to a multiple of U_{eq}(C) with 1.5 for CH_3 and 1.2 for C-H units, respectively. Additional data collection and refinement details, including description of disorder (where present) are described below. Complete crystallographic data, in CIF format, have been deposited with the Cambridge Crystallographic Data Centre. CCDC 2036712-2036715 contain the supplementary crystallographic data for this paper. These data can be obtained free of charge from The Cambridge Crystallographic Data Centre via www.ccdc.cam.ac.uk/data_request/cif

1: The two perchlorate anions were refined as disordered over each of two slightly rotated orientations. The major and minor moieties were restrained to have similar geometries for both sites. U^{ij} components of ADPs for disordered atoms closer to each other than 2.0 Å were restrained to be similar. Subject to these conditions the occupancy ratios refined to 0.760(11) to 0.240(11) (for Cl1), and to 0.776(8) to 0.224(8) (for Cl2).

2: Two perchlorate anions were refined as disordered over each of two slightly rotated orientations. The major and minor moieties were restrained to have similar geometries for both sites. ADPs of O1B and O1D and of O4B and O4D were constrained to be identical. U^{ij} components of ADPs for all disordered atoms closer to each other than 2.0 Å were restrained to be similar. Subject to these conditions the occupancy ratios refined to 0.624(8) to 0.376(8) (for Cl2A/Cl2C), and to 0.944(2) to 0.056(2) (for Cl1B/Cl1D).

3: One of the two perchlorate anions was refined as disordered over two slightly rotated orientations. The major and minor moieties were restrained to have similar geometries for both sites. U^{ij} components of ADPs for disordered atoms closer to each other than 2.0 Å were restrained to be similar. Subject to these conditions the occupancy ratios refined to 0.392(6) to 0.608(6).

4: The butyl amine moiety is disordered over two positions. The major and minor moieties were restrained to have similar geometries for both sites. U^{ij} components of ADPs for disordered atoms closer to each other than 2.0 Å were restrained to be similar. Subject to these conditions the occupancy ratios refined to 0.706(4) to 0.294(4).

Crystal structure data tables

Table S1. Summary of crystal structure data.

Compound	**1**	**2**	**3**	**4**
Formula	$C_{25}H_{25}Cl_2CoN_7O_8$	$C_{25}H_{25}Cl_2CoN_7O_8$	$C_{24}H_{24}Cl_2CoN_8O_8$	$C_{24}H_{24}Cl_2CoN_8O_8$
Mw (g mol^{-1})	681.35	681.35	682.34	682.34
Lattice Type	triclinic	triclinic	monoclinic	monoclinic
Space Group	$P\bar{1}$	$P\bar{1}$	$P2_1/n$	$P2_1/n$
a (Å)	8.6204(4)	12.6478(5)	8.7913(6)	10.5183(5)
b (Å)	9.3772(5)	12.6576(5)	8.9936(6)	14.8727(7)
c (Å)	16.8662(8)	18.4117(7)	34.173(2)	18.1709(9)
α (°)	87.9292(19)	70.7407(15)	90	90
β (°)	85.5847(16)	89.1776(16)	91.039(2)	106.3528(19)
γ (°)	88.0790(18)	87.7734(16)	90	90
V (Å^3)	1357.80(12)	2780.48(19)	2701.5(3)	2727.6(2)
Z	2	4	4	4
ϱ_{calc} (g cm^{-1})	1.667	1.628	1.678	1.662
T (K)[a]	150(2)	150(2)	150(2)	150(2)
λ (Å) [Mo Kα]	0.71073	0.71073	0.71073	0.71073
μ (mm^{-1})	0.894	0.873	0.899	0.891
S (GOF)	1.062	1.048	1.050	1.029
R(F_o), wR(F_o^2)	0.0588, 0.1015	0.0821, 0.1227	0.0725, 0.1207	0.0803, 0.1252

Table S2. Selected bond lengths for **1**-**4**.

1		**2**		**3**		**4**	
Co1-N1	1.961(1)	Co1A-N1A	1.951(1)	Co1-N1	1.947(2)	Co1-N1	1.931(2)
Co1-N2	1.907(1)	Co1A-N3A	1.910(2)	Co1-N4	1.902(2)	Co1-N3	1.911(1)
Co1-N5	1.905(1)	Co1A-N5A	1.906(1)	Co1-N6	1.901(2)	Co1-N5	1.910(1)
Co1-N6	1.936(1)	Co1A-N6A	1.933(2)	Co1-N7	1.925(3)	Co1-N7	1.948(1)
Co1-N7	2.125(1)	Co1A-N7A	2.159(2)	Co1-N8	2.116(3)	Co1-N8	2.124(2)
		Co1B-N1B	1.945(1)			Co1-O1	
		Co1B-N3B	1.907(2)				
		Co1B-N5B	1.903(1)				
		Co1B-N6B	1.924(2)				
		Co1B-N7B	2.144(2)				

Table S3. Selected bond angles for **1** and **2**.

1		**2**	
N1-Co1-N7	94.71(5)	N1A-Co1A-N3A	83.79(6)
N2-Co1-N5	92.02(5)	N1A-Co1A-N5A	159.90(6)
N2-Co1-N6	175.12(5)	N1A-Co1A-N6A	100.79(6)
N2-Co1-N7	90.46(5)	N1A-Co1A-N7A	95.76(6)
N5-Co1-N6	83.77(5)	N3A-Co1A-N5A	92.50(6)
N5-Co1-N7	105.18(5)	N3A-Co1A-N6A	175.00(6)
N6-Co1-N7	88.25(5)	N3A-Co1A-N7A	86.60(6)
		N5A-Co1A-N6A	83.87(6)
		N5A-Co1A-N7A	103.76(6)
		N6A-Co1A-N7A	90.92(6)
		N1B-Co1B-N3B	84.21(6)
		N1B-Co1B-N5B	159.99(6)
		N1B-Co1B-N6B	99.75(6)
		N1B-Co1B-N7B	95.16(6)
		N3B-Co1B-N5B	92.96(6)
		N3B-Co1B-N6B	175.75(6)
		N3B-Co1B-N7B	87.59(6)
		N5B-Co1B-N6B	83.84(6)
		N5B-Co1B-N7B	104.53(6)
		N6B-Co1B-N7B	90.50(6)

Table S4. Selected bond angles for **3** and **4**.

3.		**4**	
N1-Co1-N4	83.69(8)	O1-Co1-N1	89.07(6)
N1-Co1-N6	160.54(9)	O1-Co1-N3	87.48(6)
N1-Co1-N7	100.35(8)	O1-Co1-N5	93.95(6)
N1-Co1-N8	95.22(8)	O1-Co1-N7	78.13(6)
N4-Co1-N6	92.71(9)	O1-Co1-N8	173.83(6)
N4-Co1-N7	175.42(9)	N1-Co1-N3	84.03(7)
N4-Co1-N8	89.24(8)	N1-Co1-N5	175.68(7)
N6-Co1-N7	84.18(9)	N1-Co1-N7	99.63(7)
N6-Co1-N8	103.86(9)	N1-Co1-N8	88.31(7)
N7-Co1-N8	88.24(8)	N3-Co1-N5	92.99(7)
		N3-Co1-N7	165.03(7)
		N3-Co1-N8	97.80(7)
		N5-Co1-N7	84.05(6)
		N5-Co1-N8	88.99(7)
		N7-Co1-N8	96.81(7)

EPR spectra and simulation parameters

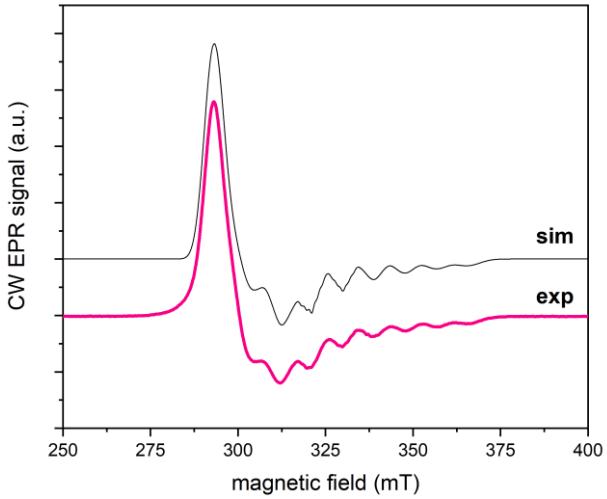

Figure S28. Experimental and simulated CW X-band EPR spectra for **O-CAT** in 1:1 CH_3CN:CH_2Cl_2.

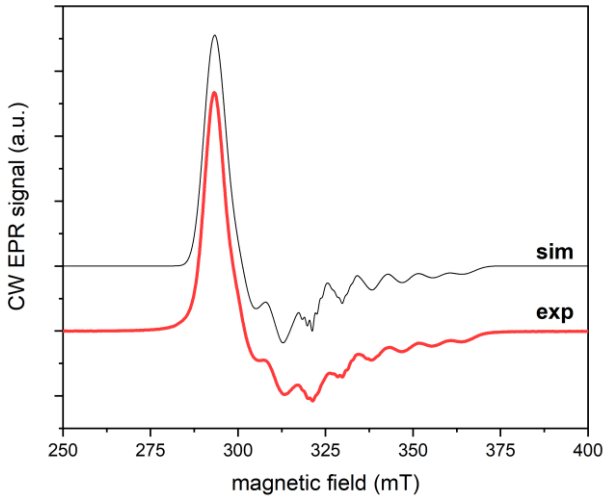

Figure S29. Experimental and simulated CW X-band EPR spectra for **1** in 1:1 CH_3CN:CH_2Cl_2.

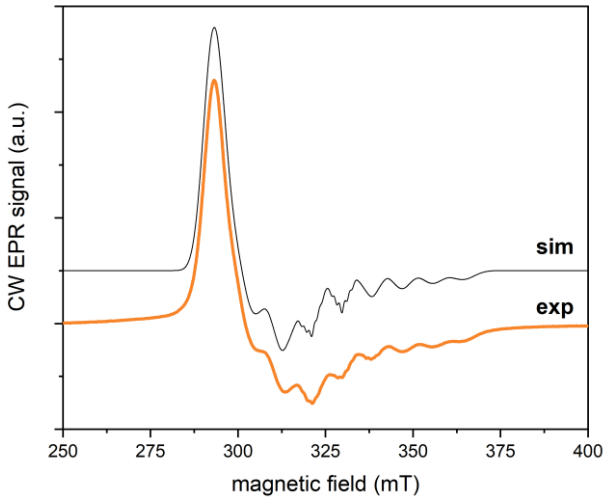

Figure S30. Experimental and simulated CW X-band EPR spectra for **2** in 1:1 CH_3CN:CH_2Cl_2.

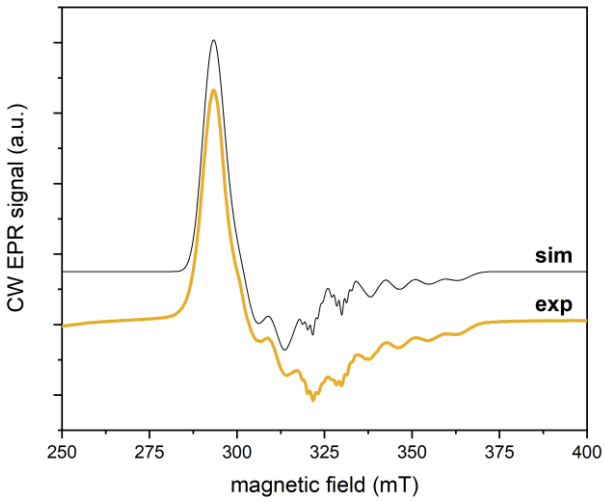

Figure S31. Experimental and simulated CW X-band EPR spectra for **3** in 1:1 CH_3CN:CH_2Cl_2.

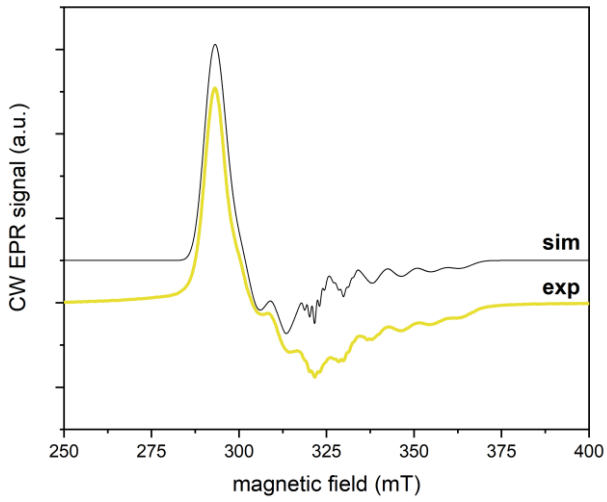

Figure S32. Experimental and simulated CW X-band EPR spectra for **4** in 1:1 CH_3CN:CH_2Cl_2.

Table S5. Summary of EPR simulation parameters. Note, the sign of the hyperfine coupling constants (HFCs) can not be determined from the EPR spectra, thus only the magnitude is given.

	g-tensor	^{59}Co HFC (MHz)	^{14}N HFC (MHz); two equivalent
O-CAT	2.260, 2.214, 2.025	45, 82, 252	38, 40, 40
1	2.262, 2.214, 2.027	45, 82, 244	38, 40, 40
2	2.262, 2.214, 2.027	45, 82, 245	38, 40, 40
3	2.266, 2.214, 2.027	45, 82, 235	38, 40, 40
4	2.267, 2.214, 2.027	45, 82, 235	38, 40, 40

References

1. Bruker *Apex3 v2019.1-0, SAINT V8.40A*, Bruker Nano Inc.: Madison, WI, USA, **2019**.
2. Krause, L.; Herbst-Irmer, R.; Sheldrick, G.M.; Stalke, D. Comparison of silver and molybdenum microfocus X-ray sources for single-crystal structure determination. *J. Appl. Crystallogr.* **2015**, *48*, 3-10, doi:10.1107/S1600576714022985.
3. Sheldrick, G. A short history of SHELX. *Acta Crystallographica Section A* **2008**, *64*, 112-122, doi:10.1107/S0108767307043930.
4. Sheldrick, G. Crystal structure refinement with SHELXL. *Acta Crystallographica Section C* **2015**, *71*, 3-8, doi:10.1107/S2053229614024218.
5. Hübschle, C.B.; Sheldrick, G.M.; Dittrich, B. ShelXle: a Qt graphical user interface for SHELXL. *J. Appl. Crystallogr.* **2011**, *44*, 1281-1284, doi:10.1107/S0021889811043202.